Pharmaceutical Technology Division
Department of Pharmacy
University of Helsinki
Finland

Near-Infrared Reflectance Spectroscopy in the Measurement of Water as a Part of Multivariate Process Monitoring of Fluidised Bed Granulation Process

by

Jukka Rantanen

Academic Dissertation

To be presented, with the permission of
the Faculty of Science of the University of Helsinki,
for public criticism in Auditorium 1 at Viikki Infocentre (Viikinkaari 11A)
on November 11th, 2000, at 12 noon

Helsinki 2000

Supervisor: Professor Jouko Yliruusi
                Division of Pharmaceutical Technology
                Department of Pharmacy
                University of Helsinki
                Finland

Reviewers: Professor Risto Kostiainen
                Division of Pharmaceutical Chemistry
                Department of Pharmacy
                University of Helsinki
                Finland

                Dr. Tech. Kari Aaljoki
                Neste Engineering Oy
                Finland

Opponent: Professor Peter York
                Professor of Physical Pharmaceutics
                Pharmaceutical Technology
                School of Pharmacy
                University of Bradford
                UK

ABSTRACT

The interest for *in-line* analysis during pharmaceutical unit operations has increased. The recent developments within process analytical chemistry enable the application of *non-invasive* measurement techniques. Near-infrared (NIR) spectroscopy is widely applied for *in-line* analysis within various unit operations in the field of chemical industry. Low absorptivities in NIR region enable the analysis with no sample preparation using the reflectance mode.

The process control and end-point detection of pharmaceutical wet granulation has not traditionally based on the direct, *in-line* measurements. The aim of the present study was to investigate the use of NIR spectroscopy for *in-line* moisture measurement during fluidised bed granulation process, and further, to integrate the NIR set-up as a part of granulator automation used for multivariate process monitoring. The *in-line* moisture measurement was performed using a four-wavelength NIR set-up. The *off-line* evaluation of wet-massing behaviour of the materials was performed using FT-NIR spectrometer.

Reliable process control combined with data logging can be used for analysing the fluidised bed granulation process. NIR spectroscopy creates a novel tool for *in-line* measurement of water. The *off-line* evaluation of materials enabled the identification of different energetic states of water in solids of pharmaceutical interest. Therefore, the future work should focus on the fast and simultaneous detection at a large number of wavelengths. The multivariate process monitoring tools used (principal component analysis and self-organizing map) can be applied to visualisation of wet granulation process. The methods are able to present the state of the granulation process and the subtle differences between various batches.

TABLE OF CONTENTS

List of abbreviations

ANNs	artificial neural networks
COGS	cost of goods sold
E	residual matrix
GAMP	Good Automated Manufacturing Practice
h	Planck's constant
I	intensity of reflectance
k	force constant (Eqs. 1 and 3)
k	absorption coefficient (Eq. 4)
NIR	near-infrared
OPD	optical data
P	loadings matrix
PAC	process analytical chemistry
PCA	principal component analysis
PID	proportional-integral-derivative
R	reflectance
s	scattering coefficient
SCADA	supervisory control and data acquisition
SOM	self-organizing map
SUPAC	scale-up and post-approval changes
SW-NIR	short wavelength near-infrared
T	scores matrix
URS	User Requirements Specifications
v	quantum number
X	process matrix

Greek letters

α	constant in training of SOM
v	frequency
$\tilde{v}_1$	frequency related to symmetric stretching vibration
$\tilde{v}_2$	frequency related to bending vibration
$\tilde{v}_3$	frequency related to asymmetric stretching vibration
μ	reduced mass

List of original publications

This thesis is based on the following original papers, which are referred to in the text by the Roman numerals I-VI.

I   Rantanen, J., Lehtola, S., Rämet, P., Mannermaa, J-P and Yliruusi, J., 1998. On-line monitoring of moisture content in an instrumented fluidized bed granulator with a multi-channel NIR moisture sensor, *Powder Technology* **99** 163-170.

II   Rantanen, J., Antikainen, O., Mannermaa, J-P and Yliruusi, J., 2000. Use of near-infrared reflectance method for measurement of moisture content during granulation, *Pharmaceutical Development and Technology* **5** 209-217.

III   Rantanen, J., Känsäkoski, M., Suhonen, J., Tenhunen, J., Lehtonen, S., Rajalahti, T., Mannermaa, J-P and Yliruusi, J., 2000. Next generation fluidized bed granulator automation, *AAPS PharmSciTech* **1** (2), http://www.pharmscitech.com/.

IV   Luukkonen, P., Rantanen, J., Mäkelä, K., Räsänen, E., Tenhunen, J. and Yliruusi, J., 2000. Characterization of wet massing behavior of silicified microcrystalline cellulose and α-lactose monohydrate using near infrared spectroscopy, *Pharmaceutical Development and Technology* (accepted).

V   Rantanen, J., Räsänen, E., Mannermaa, J-P and Yliruusi, J., 2000. In-line moisture measurement during granulation with a four wavelength near infrared sensor: an evaluation of particle size and binder effects. *European Journal of Pharmaceutics and Biopharmaceutics* **50** 271-276.

VI   Rantanen, J., Laine, S., Antikainen, O., Mannermaa, J-P, Simula, O. and Yliruusi, J., 2000. Visualization of fluid bed granulation with self-organizing maps. *Journal of Pharmaceutical and Biomedical Analysis* (accepted).

1. INTRODUCTION

Understanding the physicochemical phenomena during manufacture of pharmaceutics is of importance. Recent developments of drug delivery systems and the increasing amount of new drug molecules have imposed new challenges for pharmaceutical technology. The advancements in the field of particle engineering have established a possibility to create particles with defined characteristics. By this means, the number of complex unit operations in the field of pharmaceutics will increase. In the simplified flow chart of manufacture of a traditional solid dosage form, there are several sequential unit operations (Fig. 1). Traditionally, the level of automation of pharmaceutical unit operations has been low. Further, the developments of process analytical chemistry (PAC) have not been widely utilised. This has been due to the high documentation requirements of new process measurement and control practices. However, the development of PAC together with increasing level of automation creates tools for understanding the physicochemical phenomena during these sequential unit operations. Therefore, the in-process control of pharmaceutical manufacture is improved and the degree of safety is increased. The implementation of new manufacturing technologies widens the traditional set of sequential unit operations. The novel PAC tools together with robust automation will ensure the high degree of quality.

The vast amount of different dosage forms and formulations complicates the understanding of the manufacture of pharmaceutics. The recent development within process analytics together with progression of computer performance offers new possibilities. However, there have not been valid analytical methods available for understanding the phenomena during manufacture of pharmaceutics. The application of different data mining tools is needed in order to understand the multidimensional problems in the pharmaceutical field.
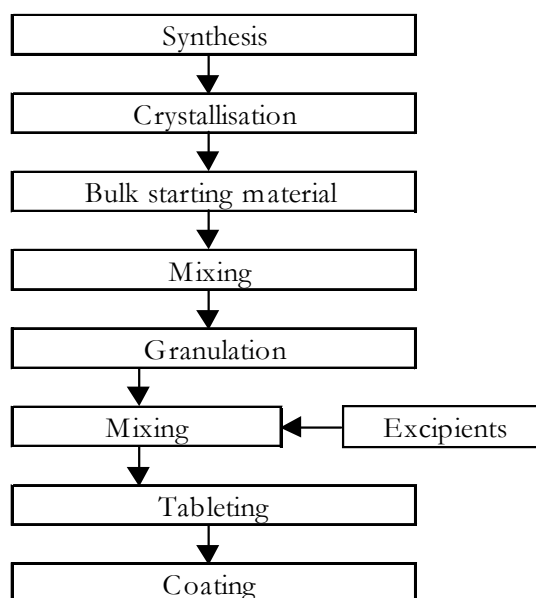

Figure 1. The manufacture of traditional solid dosage form.

Formulation and processing changes during development, manufacture and product optimisation can influence the performance of a pharmaceutical formulation. The scientific foundation related to scale-up and post approval changes (SUPAC) has been defined in co-operation between authorities and academy (Skelly et al., 1993). The development of process analytical chemistry will create a tool for SUPAC, when the behaviour of formulation during processing can be verified between different batch sizes, sites of manufacture or manufacturing processes. Further, production costs (cost of goods sold, COGS) have become an increasingly important factor in pharmaceutical industry (Vrettos and Hofmann, 1996). The pressure to reduce health care costs is increasing, which results in a need for efficient production. Vrettos and Hofmann (1997) have introduced five main clusters in optimising the manufacturing structure of an international pharmaceutical company. First, the existing production should be redistributed over a reduced number of sites. The existing technology capacities should be consolidated and optimised. Third, the existing capacities and volume to be produced should be co-ordinated. The technology should be controlled by focusing investment. Last, exploit synergies for overhead functions and scale effects for variable functions.

Thus, the proper understanding of the whole production cycle creates a base for a profitable manufacturing structure and a high degree of quality. A central part of optimising production is increasing the level of automation. Developing a functional automation system requires new measuring techniques; new *in-line* measuring devices are needed (Callis et al., 1987; Beebe et al., 1993; Blaser et al., 1995; Hassel and Bowman, 1998; Workman et al., 1999). Solid-water interactions are one of the fundamental issues in the pharmaceutical technology. State of water in solid material may be characterised using x-ray diffraction, microscopic methods, thermal analysis, vibrational spectroscopy, and nuclear magnetic resonance spectroscopy (Brittain, 1999). Traditionally, the control of fluidised bed granulation has based on indirect measurements. These control methods applied utilise the properties of process air (Schæfer and Wørts, 1978). The non-destructive character of vibrational spectroscopy techniques, such as near infrared (NIR), makes them novel tools for *in-line* quality assurance (Workman, 1993; Axon et al., 1998). NIR has been widely used for the measurement of water in various applications (Osborne et al., 1993). NIR can be applied for both quantitative analysis of water and for determining the state of water in solid material. This gives a tool for understanding the physicochemical phenomena during manufacture of pharmaceutics.

2. THEORY

2.1 Near-infrared spectroscopy

2.1.1 General aspects of near-infrared spectroscopy

The history of near-infrared (NIR) spectroscopy dates back to the studies by Herschel (Herschel, 1800). The measurement of heat energy beyond the red portion of the visible spectrum was performed. The visible area covers the electromagnetic spectrum from about 380 to 760 nm, and the NIR region is between 760 and 2600 nm. However, it was not until the Second World War that the development of NIR instrumentation enabled the practical applications of this region of the spectrum. The modern NIR analysis was developed in the 1950s by the work of a group at USDA (United States Department of Agriculture), headed by Karl Norris (Osborne et al., 1993). They evaluated the physicochemical methods for rapid quality control of agricultural commodities. One of their findings was that the non-destructive reflectance NIR spectra of biological samples could be obtained. This gave rise to a wide use of NIR in the agricultural field.

Other branches of chemical industry have also applied NIR for various applications. Petrochemical, pulp and paper, and pharmaceutical industry have taken advantage over characteristics of NIR (Workman, 1993). The field of astrophysics has also widely applied this spectroscopic region. One feature of NIR is that the applications have been ahead of theoretical aspects. This has hindered the general approval of NIR, e.g. in the pharmaceutical field. However, the pharmacopoeias have recently defined some characteristics of the analysis with NIR (Ph. Eur. 3rd Ed., 1997; USP XXIV, 2000).

2.1.2 Physicochemical background

Mechanical model of the vibration of diatomic molecular bond can be considered as two masses (m_1 and m_2) connected to each other by a spring. A specific frequency (v_0) for a vibration of a pair of covalently bound atoms is

$$v_0 = \frac{1}{2\pi}\sqrt{\frac{k}{\mu}} \tag{1}$$

where k is force constant and μ is reduced mass. The molecules vibrate at frequencies corresponding to wavelengths in the infrared region. By solving quantum mechanical wave function for a simple harmonic oscillator, the discrete amount of energies for vibration can be calculated by

$$E_v = (v + \tfrac{1}{2})hv_0 \qquad\qquad (2)$$

where v is the vibrational quantum number (0, 1, 2, 3, …) and h is Planck's constant. The interaction between the electromagnetic radiation and the chemical bond is quantised. Thus, the promotion to the first excited state ($v = 1$) requires the energy ΔE (Eq. 3).

$$\Delta E = hv_0 = \frac{h}{2\pi}\sqrt{\frac{k}{\mu}} \qquad\qquad (3)$$

This approach explains quite well the mid-IR absorption bands due to the fundamental modes of molecular vibration ($\Delta v = \pm 1$). The bands observed at the NIR region are overtones ($\Delta v = \pm 2, \pm 3, ...$), and combinations of fundamental vibrations and overtones. The probabilities of these transitions are lower than those of the fundamental transitions, which can be utilised by the use of reflectance mode in NIR spectroscopy. Most materials appear "black" at the wavelengths longer than 2500 nm due to the level of absorption of the fundamental bands. One advantage of the use of the NIR region is the non-destructive nature of the measurements, which enables the direct measurement from, e.g., process stream.

Vibration can be described as either stretching or bending. Vibration involving a change in the interatomic distance is known as stretching, and vibration involving a change in the bond angle is known as bending. The fundamental vibrations are $\tilde{v}_1$ (symmetric stretching), $\tilde{v}_2$ (bending), and $\tilde{v}_3$ (asymmetric stretching). The real molecules do not perfectly obey the law of harmonic vibration. The intensity of overtone and combination bands depends on the degree of anharmonicity, and these different modes of vibration give rise to bands observed at the NIR region. The absorption of the radiation at the near-infrared region is attributed to the low mass of the hydrogen atom. The bonds involving hydrogen vibrate with large amplitude. Therefore, the absorption bands observed at the NIR region arise from overtones of stretching vibrations involving functional groups with hydrogen atom or combinations involving stretching and bending modes of vibration of these groups. Most of the NIR bands observed

involve CH, OH, NH and SH bonds. The absorption bands of water in the NIR region occur at 760 nm, 970 nm, 1190 nm, 1450 nm, and 1940 nm (Curcio and Petty, 1951; Buijs and Choppin, 1963). The band around 1940 nm is caused by a combination of OH stretching and bending vibrations ($\widetilde{v}_2 + \widetilde{v}_3$) (Choppin and Downey, 1972), and it is often applied for process analytical applications (Osborne et al., 1993). The bands around 1450 nm, 970 nm, and 760 nm are issued from the first to the third overtone of OH stretching vibrations, respectively. Further, the band at 1190 nm is a combination band ($\widetilde{v}_1 + \widetilde{v}_2 + \widetilde{v}_3$) (Buijs and Choppin, 1963). Recently, the short-wavelength NIR (SW-NIR) region (760 nm and 970 nm bands have been applied for high moisture systems (Reeves, 1994; Kemppainen et al., 1999). The lower absorption and the higher penetration depth enable the analysis of high moisture levels at the SW-NIR.

In reflectance spectroscopy the light reflected from the sample is measured. The incident beam of light (I) is divided into two parts, as shown in Fig. 2: the transmitted light (T) and the reflected light (R). The reflected light generally consists of two components, specular and diffuse component. The specular (mirror-like) component occurs at the interface (refractive indices n_1 and n_2), and it contains only little information about the chemical composition
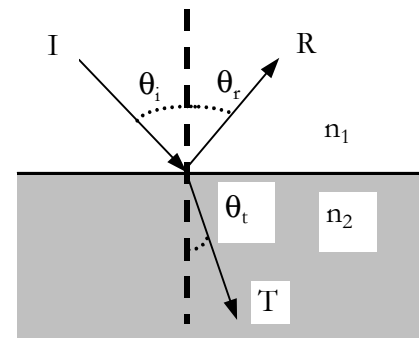

Figure 2. Beam of light on the interface of two media.

of the sample. The specular component for the boundary between two media can be described by Snell's law and the Fresnel equations (Kortüm, 1969). The NIR spectroscopy is mainly based on the diffuse component of the reflected light. When it comes to reflectance from a matte surface, e.g. powder, the boundary between two media may be considered as series of interfaces orientated randomly. Part of the light may be transmitted through the first interface, and therefore absorption may occur. The diffuse reflected light is emerged by random reflections, refractions and scatter inside the sample. Further, more transmission and absorption may occur at other interfaces. The exact path for propagating light is extremely difficult to model. Only experimental theories have been proposed. Kubelka-Munk function (Eq. 4) for a case with infinite thickness of sample describes the power of reflected light by

$$f(R) = \frac{k}{s} = \frac{(1-R)^2}{2R} \tag{4}$$

where k is absorption coefficient and s is scattering coefficient. This function may be related to concentration, c, of the absorbent ($c \propto f(R)$). In practical applications, the apparent absorbance A is applied (Eq. 5).

$$A = \log \frac{1}{R} \qquad\qquad (5)$$

This apparent absorbance value is expected to be related to the concentration of the absorbent ($c \propto \log 1/R$).

However, numerous factors of the sample affect the detected reflectance signal. The particle size and shape distributions, bulk density, texture of the surface and sample temperature affect the determinations with NIR (Williams, 1987). Norris and Williams (1984) evaluated the particle size effects with cereals. Various mathematical treatments have been suggested for modelling the particle size data with NIR spectra (Ciurczak et al., 1986; Ilari et al., 1988; Bull, 1990; Bull, 1991; Frake et al., 1998; Rantanen and Yliruusi, 1998; O'Neil et al., 1998; O'Neil et al., 1999). Berntsson et al. (1999) evaluated methods for the determination of the effectively sampled mass per unit area. Further, the analysis of water is affected by the hydrogen bonding environment of the water molecules. Fornés and Chaussidon (1978) found the combination band of water ($\widetilde{\nu}_2 + \widetilde{\nu}_3$) around 1940 nm to be centered at 2008 nm (4980 cm^{-1}) with ice (each water molecule forms four hydrogen bonds with surrounding water molecules). With increasing temperature and melting of ice, the absorbance maximum with liquid water occurs at lower wavelengths (an apparent isosbestic point at 1957 nm, 5110 cm^{-1}). Part of hydrogen bonds is broken and the median interaction energy of –OH bond increases, while temperature increases. In the case of water vapour (no hydrogen bonds between water molecules), the $\widetilde{\nu}_2 + \widetilde{\nu}_3$ band occurs at 1875 nm (5332 cm^{-1}) (Choppin and Downey, 1972). This band has been resolved into three Gaussian shaped component bands, s_0, s_1, and s_2 (neither, one, or two –OH groups hydrogen bonded, respectively). The hydrogen bond formation through oxygen atom has been considered to have little or no influence on the vibration of –OH bond (Buijs and Choppin, 1963; Fornés and Chaussidon, 1978). However, Maeda et al. (1995) resolved the 1450 nm band (first overtone) to five component bands, s_0, s_1, s_2, s_3, and s_4 (neither, one, two, three or four hydrogen bonds, respectively). The median interaction energy may also be affected by mixing water with ionic compound or various solvents (Choppin and Buijs, 1963;

Choppin and Violante, 1972; Choppin and Downey, 1972). This gives a window to evaluate the portion of molecules in different hydrogen bonding environments. NIR has been applied for studying the nature of water-solid interactions within various materials (Iwamoto et al., 1987; Delwiche et al., 1991; Buckton et al., 1998; Švedas, 2000).

2.1.3 Spectral data analysis

Development of computer performance together with instrumental breakthroughs enables the reliable detection of spectrum. The development of computer performance enables the application of demanding mathematical processing methods. This is one reason for the increasing use of NIR spectroscopy. As described before, the NIR spectrum is affected by the physicochemical properties of the sample (Williams, 1987). This can be utilised by applying NIR for the determination of physical parameters, e.g. particle size. However, in quantitative analysis these effects should be minimised. The linearisation of the detected reflectance signal to Kubelka-Munk units (Eq. 4) or apparent absorbance (Eq. 5) is the first step of spectral analysis. In the NIR region, the absorption bands are broad and overlapping. Further, the effects of physical properties of the sample to the NIR spectra disturb the quantitative analysis. Mathematical pre-processing of the spectra is needed to provide relevant chemical information of the absorbent (Martens and Næs, 1993). The methods applied include derivatization of spectra, normalisation, multiplicative scatter correction (MSC), standard normal variate (SNV), de-trending (DT), Fourier transform (FT), principal component analysis (PCA), orthogonal signal correction (OSC), and wavelet compression. Savitzky and Golay (1964) introduced algorithms, which may be used for programming the calculation of the derivatives, e.g. from NIR spectra. Normalisation of spectra may be performed, e.g., to unit length, to minima or maxima value of spectra, to a certain low absorbance value at the spectra. MSC by Martens and co-workers (Geladi et al., 1985) can be used for separating the chemical absorption from physical light scatter. The fit for each individual spectrum and the mean spectrum is performed by least squares

$$x_i = a_i + b_i \bar{x}_j + e_i \qquad (6)$$

where x_i is an individual spectrum i, $\bar{x}_j$ the mean spectrum of the data set, and e_i the residual spectrum. The constants a_i (offset) and b_i (slope) are used to correct each value of the spectrum i, as follows

$$x_{i,MSC} = \frac{x_i - a_i}{b_i}. \tag{7}$$

SNV may also be applied to remove the particle size effects by

$$x_{ij,SNV} = (x_{ij} - \overline{x}_i)/\sqrt{\frac{\sum_{j=1}^{p}(x_{ij} - \overline{x}_i)^2}{p-1}} \tag{8}$$

where $x_{ij,SNV}$ is the transformed element of an individual spectrum, x_{ij} the original element of an individual spectrum, $\overline{x}_i$ the mean spectrum i and p the number of variables in the spectrum (Barnes et al., 1989). De-trending is performed by fitting a second-order polynomial to the baseline of the spectrum, and, by subtracting this polynomial from spectrum (Barnes et al., 1989). The feature reduction methods, such as FT, PCA, OSC, wavelet and neural networks, require effective computer performance. Therefore, the recent development of computers has enabled the application of these methods (Wold et al., 1998a; Trygg and Wold, 1998; Sjöblom et al., 1998). Pre-processing methods may also be used as combinations. Candolfi et al. (1999a) evaluated the effect of pre-processing of NIR spectra to the pattern recognition of excipients.

2.1.4 Advantages and disadvantages of near-infrared spectroscopy

Low absorptivities in the NIR region enable the analysis with no sample preparation using the reflectance mode. Consequently, advantages over traditional wet chemistry methods are gained by using the NIR spectral region. There is no sample preparation step, and the time needed per analysis is reduced. The application of fiber optics enables the process analytical applications, and the analysis may be transferred to production site.

The bands observed at the NIR region are overtone and combination bands, and the selectivity of NIR is relatively poor in comparison with, e.g., mid-IR region. Thus, the bands at the NIR region are broad and overlapping. Therefore, the spectral analysis requires application of mathematical tools, which require experienced personnel and computer performance. The transformation of spectra between different instruments is not straightforward.

However, the accuracy achieved with NIR moisture measurement (standard error of performance of 0.5%) has been considered acceptable for in-process moisture specification (Frake et al., 1997). The time needed for sampling and moisture

measurement with traditional methods (e.g. loss on drying, Karl Fischer titration) is remarkably higher than the time needed for *on-line* or *in-line* analysis with NIR.

2.2 Applications of near-infrared spectroscopy

2.2.1 Definitions

The border between process analytical chemistry (PAC) and more traditional laboratory analysis is quite ambiguous. The terms *in-line, on-line, at-line, off-line, non-invasive* are often referred to in literature. Definitions of these classes are given (Callis et al., 1987; Beebe et al., 1993; Blaser et al., 1995; Hassel and Bowman, 1998; Workman et al., 1999): *in-line*, the sample interface is located in the process stream; *on-line*, automated sampling and sample transfer to an automated analyser; *at-line*, manual sampling with local transport to analyser located in manufacturing area; *off-line*, manual sampling with transport to remote or centralised laboratory.

Further, process analysis is moving into plant environment. There is a need for rapid *non-invasive* analytical methods. *In-line* study of the state of the process increases the production efficiency and the degree of safety. New process automation systems and data visualisation tools support this trend. On the other hand, combination of process analytics and data visualisation tools creates new tools for understanding the physicochemical phenomena during processing.

2.2.2 *Off-line* applications

During the past decade, the pharmaceutical industry has adopted NIR in various applications (Morisseau and Rhodes, 1995; Blanco et al., 1998). Morisseau and Rhodes (1997) summarised the main pharmaceutical applications of near infrared spectroscopy within solid dosage form manufacture. The measurement of water was one of the first pharmaceutical applications of NIR (Sinsheimer and Poswalk, 1968). Recently, detection of moisture in freeze-dried solids (Kamat et al., 1989; Last and Prebble, 1993; Jones et al., 1993; Derksen et al., 1998) and in other solid materials (Plugge and van der Vlies, 1993; Dreassi et al., 1996; Blanco et al., 1997) has been reported. The polymorphic form of the drug substance may be determined (Aldridge et al., 1996; Luner et al., 2000).

Identification and quality control of raw materials is an everyday analytical problem in pharmaceutical industry. The publication of the NIR Monograph (Ph. Eur.

3rd Ed., USP) has increased general interest on this method (Leiper et al., 1998). Current mid-IR pharmacopoeial identity test does not include information of the normal chemical and physical distribution occurring with material in manufacturing environment. The issues of sample preparation, mathematical treatment, and definition of 'identified sample' has been discussed both by the regulatory (Reader's tribune/Pharmeuropa, 1999; Reader's tribune/Pharmeuropa, 2000) and by academy (Plugge and van der Vlies, 1996; Blanco et al., 1998; Blanco et al., 1999; Yoon et al., 1998; Yoon et al., 1999; Berntsson et al., 1999; Candolfi et al., 1999a; Candolfi et al., 1999b; Moffat et al., 2000).

2.2.3 Process analytical applications (*at-line*, *on-line* and *in-line*)

NIR has been widely applied to different applications within the manufacture of solid dosage form (Fig. 3). Wet granulation of pharmaceutics was the first process analytical application of NIR in the pharmaceutical field (Watano et al., 1990; White, 1994; List and Steffens, 1996; Frake et al., 1997; Goebel and Steffens, 1998; Morris et al., 2000). Hailey et al. (1996) and Sekulic et al. (1996) interfaced NIR spectroscopy with blending process equipment and they used NIR for *on-line* blend analysis. Monitoring of the film coating process parameters has been reported by Kirsch and Drennen (1995, 1996). Andersson et al. (1999) performed *at-line* evaluation of the amount of the coating on tablets. Further, Andersson et al. (2000) described real-time analysis of film coating of pellets. Buice et al. (1995) and Berntsson et al. (1997) applied NIR for *at-line* quality control of gelatin capsules.

Another pharmaceutical PAC application area of NIR is within the synthesis of pharmaceutics. Hammond et al. (1998) used NIR to monitor the progress of the chemical reaction. Norris et al. (1997) combined NIR with principal component analysis to follow the polymorphic conversion of crystalline organic compound.
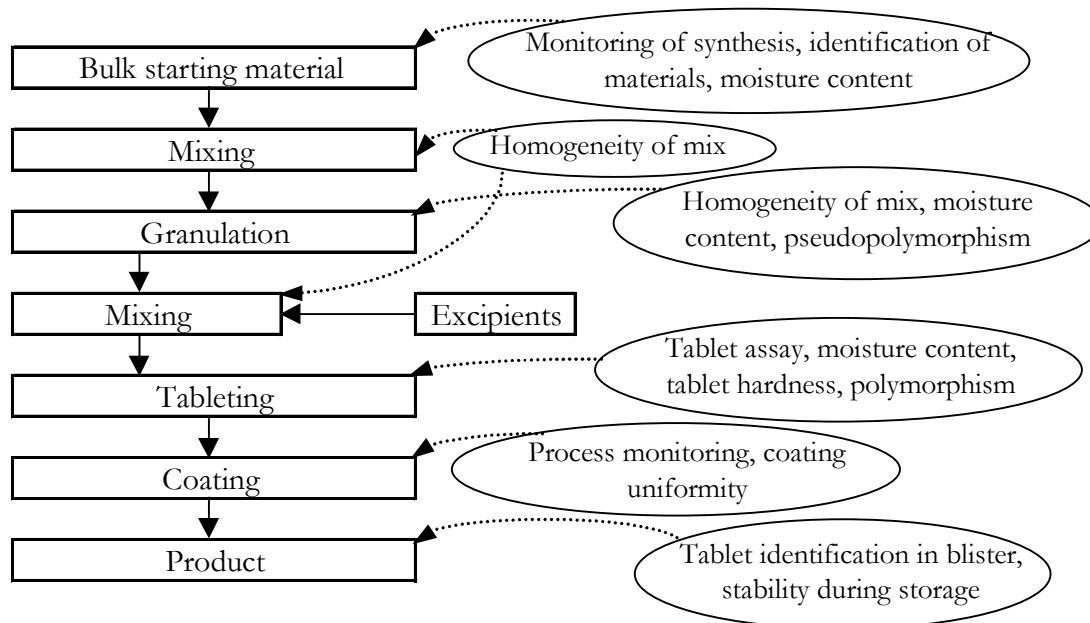
Bulk starting material → Monitoring of synthesis, identification of materials, moisture content

Mixing → Homogeneity of mix

Granulation → Homogeneity of mix, moisture content, pseudopolymorphism

Mixing ← Excipients

Tableting → Tablet assay, moisture content, tablet hardness, polymorphism

Coating → Process monitoring, coating uniformity

Product → Tablet identification in blister, stability during storage

Figure 3. The application of NIR for the analysis of different steps of manufacture of solid dosage form (modified from Han and Faulkner, 1996).

2.3 Dimension reduction tools

2.3.1 Why multivariate data analysis tools are needed

The summaries and quick overviews of data sets are easily created using statistics, such as the smallest and largest data value, the median, the mean, and the quartiles of the data set. These are valid tools for summarising small sets, and a quick overview is achieved. However, increasing the amount of variables and observations in data sets results in a large number of statistics. The ability of human mind to visualise this increasing amount of information is restricted. Therefore, new tools for understanding the structures in vast multivariate data sets are needed. Especially, in the field of pharmaceutical technology, the number of different formulations and unit operations results in a problematic field (Rowe and Roberts, 1998).

The term chemometrics is often used to describe an approach to extract chemically relevant information from data produced in chemical experiments (Wold, 1995). For example, the development of quantitative or qualitative NIR applications often requires application of multivariate models (Martens and Næs, 1993; Lavine, 1998;

Lavine, 2000). Commercial software often base on the use of chemometric methods (e.g. multivariate linear regression or methods applying principal components).

Further, the analysis of process data is difficult with traditional statistics (Kourti and MacGregor, 1995). The process with varying conditions and sequential phases (e.g. fluid bed granulation) can not be described with e.g. mean or smallest and largest data value. These statistics give only a limited view of the process. Therefore, the multivariate approach is often applied in process analytics.

The classification of data mining tools is not unambiguous. The methods applied in this thesis are presented.

2.3.2 Principal component analysis

The multivariate approach by using principal component analysis is dating back to the beginning of the 20th century (Pearson, 1901; Hotelling, 1933). Principal component analysis (PCA) is used for getting overview of data tables (their structure, similarities or dissimilarities, trends, deviating observations). Partial least squares projection to latent structures (PLS) can be used for modelling the relationship between two data matrices, X and Y. The basic idea is to calculate PCA or PLS components, also known as latent variables, that summarise the variation of the original dataset, and thus extract information from all data simultaneously. Reduction of the dimensionality from the original variables to these latent variables makes the graphical presentation of the results possible. Applications in pharmaceutical technology include development of formulation (Gabrielsson et al., 2000) and optimisation of manufacture of solid dosage form (Bergman et al., 1998). Process monitoring has been performed using methods basing on principal component analysis (Kresta et al., 1991; Nomikos and MacGregor, 1995; Kourti and MacGregor, 1995; Wold et al., 1998b; Svensson et al., 1999).

The idea of principal components may be simplified using three-dimensional example (Fig. 4). Each observation (row in the data table X) is represented by one point in the K-dimensional space (K is the number of variables). Data matrix X hence is a swarm of points in this space. The first principal component (PC$_1$) is the line in X space that best approximates the data (least squares fit). PC$_2$ improves the approximation of X as much as possible, and it is represented by a line in X space orthogonal to PC$_1$. The two principal components form a plane in the X space (a two-dimensional window into

the multidimensional space). The original points can be projected onto this plane. Scores (t) are co-ordinates in the plane and loadings (p) define the direction of the plane.
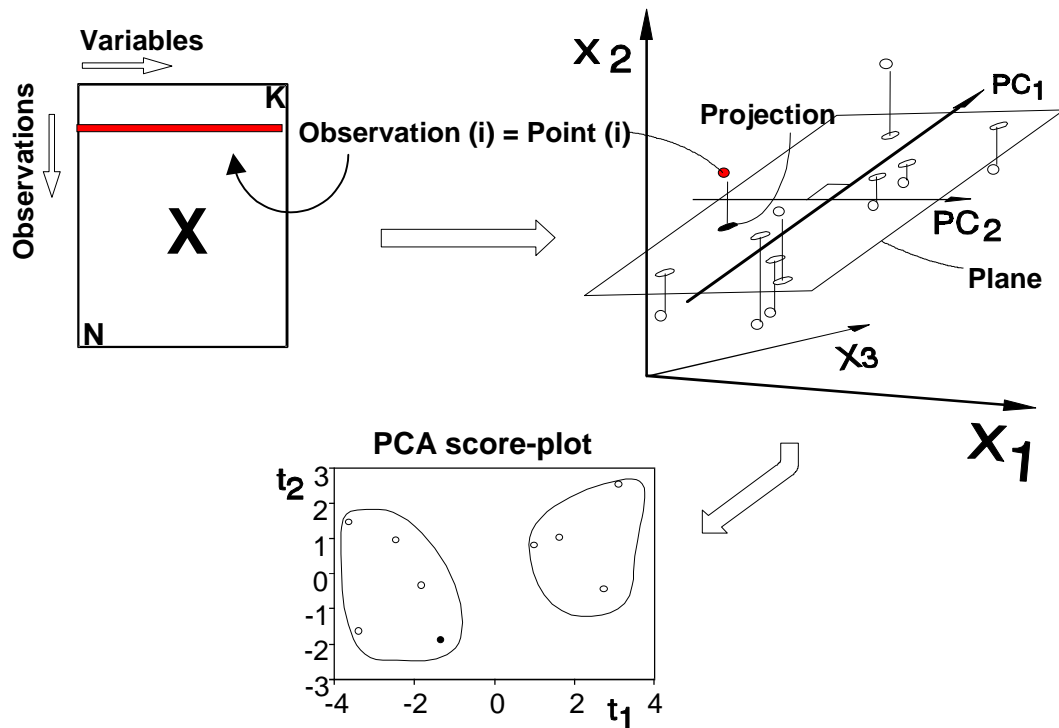

Figure 4. The three-dimensional presentation of data projection using principal components.

2.3.3 Artificial neural network

There is no simple definition for artificial neural networks (ANNs). On the one hand, these methods are considered simply as a class of mathematical algorithms. On the other hand, ANNs methods can be considered to mimic the biological nervous system found in living organisms. However, ANNs algorithms are often only inspired by biological systems, and no real uniformity exists.

ANNs trained with a teacher (target output) are known as supervised techniques. In supervised learning, the network creates a model that maps between training input matrix and the required response. Supervised learning requires the use of training targets. These techniques include e.g. back-propagation training algorithm (Fig. 5). The ANNs model is optimised by affecting the model after each training cycle. Unsupervised learning is a process when the network is able to discover similarities in its input space

without training target. No feedback from the environment (e.g., target outputs) will be needed during training, and the network can organise a topological map of the input vectors. One of the most famous unsupervised learning technique is the Kohonen algorithm, self-organizing map (SOM) (Kohonen, 1982) (Fig. 6).
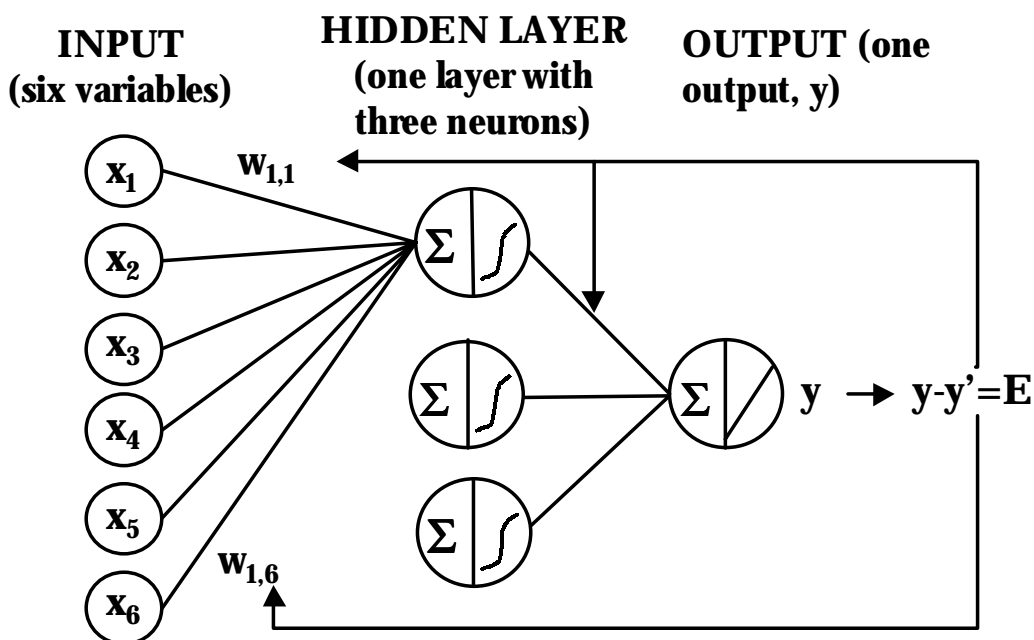

Figure 5. The back-propagation algorithm. Each input variable (x_i) is connected by corresponding weight value ($w_{m,n}$) to each neuron in hidden layer. During training phase, the training error (E) is minimised by affecting the weight values after each training cycle.

ANNs methods have been applied to pharmaceutical product development (Hussain et al., 1991; Hussain et al., 1994; Bourquin et al., 1997). The first process modelling based on ANNs in the pharmaceutical field was introduced by Murtoniemi et al. (1994a, 1994b). Watano et al. (1997a) applied ANNs for control of moisture content in fluidised bed granulation. Watano et al. (1997b) introduced also ANNs for scale-up of granulation. The central granule properties in production-scale equipment could be predicted using learning data from laboratory-scale equipment. ANNs methods have also been applied for pharmacokinetic studies; Hussain et al. (1993) introduced ANNs for predicting human pharmacokinetic parameters from animal data and Erb (1995)

predicted area under the plasma concentration-time curve using dose and demographic data as inputs. These ANNs applications have mainly used supervised learning algorithms (back-propagation).

9x9 output layer (SOM)

Weight vectors (one example included w)

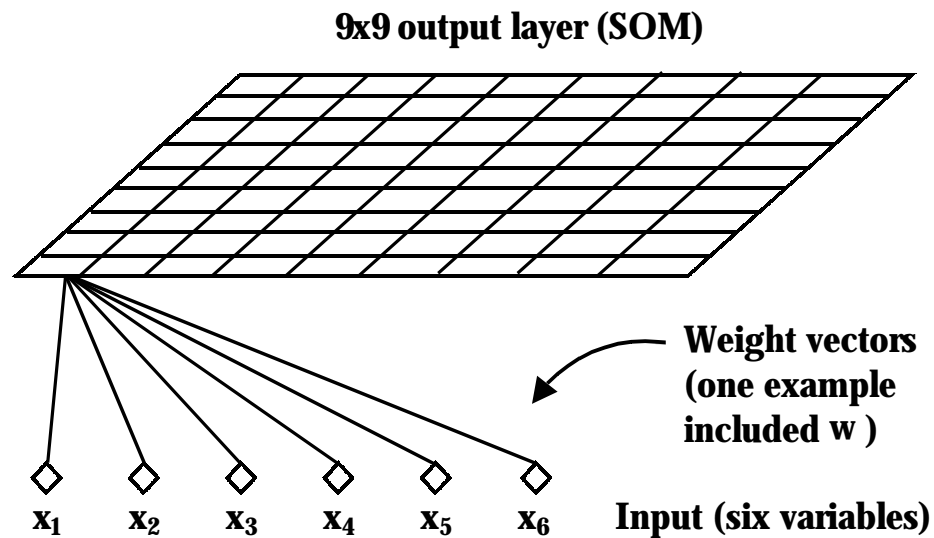x_1 x_2 x_3 x_4 x_5 x_6 **Input (six variables)**

Figure 6. Self-organizing map (SOM). During the training phase, a topological map of the input vectors is composed by finding the winning neuron for each input vector (minimum distance between input and weight vectors). Similar vectors organise to the same regions of the map after training cycle.

The applications of the Kohonen algorithm have been presented (Kohonen, 1997). An overview of process applications with SOM has been presented by Simula and Kangas (1995). A general view to process control has also been provided by Tryba and Goser (1991) and Padgett et al. (1995).

3. AIMS OF THE STUDY

Traditionally, the process monitoring of wet granulation of pharmaceutics has not based on direct, *in-line* measurements. A direct insight into the material during processing will generate a novel tool for understanding the physicochemical phenomena during processing. The aim of the present study was to investigate the use of near-infrared (NIR) spectroscopy for *in-line* moisture measurement during fluidised bed granulation process, and further, to integrate the NIR set-up as a part of granulator automation used for multivariate process monitoring. The specific aims were:

1. to investigate the use of a four-wavelength NIR set-up in fluid bed granulation of pharmaceutics, and to develop sight glass solution for *in-line* measurement

2. to study the effect of formulations with varying chemical compounds on the moisture measurement with NIR set-up

3. to understand the effect of physical factors on the moisture measurement with NIR set-up

4. to study the use of in-line NIR moisture measurement as a part of pharmaceutical process optimisation

5. to integrate the NIR set-up as a part of fluid bed granulator automation used for multivariate process monitoring.

4. EXPERIMENTAL

4.1 Materials

In the first phase of the studies, the materials applied (I, II) were 80 mesh α-lactose (Pharmatose, DMV, the Netherlands), 200 mesh α- lactose (Pharmatose, DMV, the Netherlands), mannitol (Mannitol 60, Roquette, France), microcrystalline cellulose (Emcocel 50M, Penwest Pharmaceuticals, Nastola, Finland), pregelatinized maize starch (Starch 1500, Colorcon, USA) and verapamil hydrochloride (Orion Pharma, Finland). The binders used in the granulation liquids were polyvinylpyrrolidone (Kollidon K25, BASF, Ludwigshafen, Germany, (I-III, VI); Plasdone K-25, ISP Technologies Inc., Wayne, NJ, USA, (V)) and gelatin (Orion Pharma, Finland).

Theophylline anhydrate (BASF, Ludwigshafen, Germany) and silicified microcrystalline cellulose (SMCC) (Prosolv SMCC 50, Penwest Pharmaceuticals, Nastola, Finland) were used as test materials in further development of granulator (III, V, VI). Glass ballotini (Jencons Ltd., Bedfordshire, England) of three different particle size distributions was used as a model compound in FT-NIR measurements (V).

4.2 Characterisation of materials

4.2.1 Properties of starting materials and granules

Particle size and size distributions were determined by a laser light diffractometer (Malvern 2600C droplet and particle sizer, Malvern Instruments Ltd., UK). The method of determination was particles in air (PIA).

Bulk volume was determined by pouring 50 g of material into a 250 ml glass measuring cylinder held at an angle of 45° to the horizontal while pouring. After pouring, the measuring cylinder was brought to a vertical position and the bulk volume was read. Tapped volumes were determined using a standardised tapped density tester (Erweka SVM1, Erweka GmbH, Heusenstamm, Germany) in which the glass measuring cylinder was tapped 500 times.

The true density of materials was measured using a pycnometer (Micromeritics, Model 1305, Norcross, GA, USA). The results are averages of three triplicate determinations.

Flowabilities were determined in triplicate using a Flow Time and Cone Angle Testing Instrument (Pharma Test PTG, Pharma Test, Germany). The flowability was measured as the time required for a granule sample (30 g) to flow through a 8 mm orifice.

Moisture content of materials was determined using an infrared dryer (Sartorius Thermocontrol YTC01L, Sartorius GmbH Göttingen, Germany). The samples were heated in the infrared dryer until the loss of weight was less than 0.1% in 50 seconds. The validity of the drying method was tested (I) using a recirculated air oven (Heraeus UT 6760, Germany) and a Karl Fischer titrator (Mettler DL35, Mettler-Toledo AG, Switzerland).

4.2.2 Properties of wet powder masses (IV)

The rheological profiles of the wet masses were monitored using a mixer torque rheometer (Model MTR, Caleva Ltd, Dorset, UK) similar to that described by Luukkonen et al. (1999). Dry powder was mixed in the rheometer for 3 minutes to obtain the baseline response, which was afterwards deducted from torque responses. Water was added in a single addition and the mixture was wet massed at 52 rpm for 12 minutes. All the wet massing experiments were performed in triplicate and a mean torque value and a standard deviation were calculated.

4.2.3 Properties of tablets (III)

Tablet properties (mass, dimensions, and crushing strength) were measured with an automated tablet tester (Erweka Multicheck, Erweka GmbH, Germany). Properties of twenty tablets were measured immediately after compression and another 20 were measured after 24 hours of controlled storage (35 ± 3 RH%, 24 ± 2°C).

4.3 Unit operations

4.3.1 Fluidised bed granulation (I-III, VI)

The granulations were performed in a pilot-scale fluidised bed granulator (Glatt WSG 5, Glatt GmbH, Binzen, Germany). Three sequential unit operations (mixing, spraying, and drying) were performed in same granulation chamber. This study was based on previous automation projects (Niskanen et al., 1990; Merkku et al., 1992). The critical process information describing the state of the granulation was measured (III). The flow rate and

temperature of process air were PID (Proportional-Integral-Derivative) controlled. Further, the spraying pressure and granulation liquid flow rate were user-controllable. The supervisory control and data acquisition (SCADA) system was based on FactorySuite 2000 (Wonderware Corporation, Irvine, CA, USA).

The development of the present automation was based on the User Requirements Specifications (URS, by *Good Automated Manufacturing Practice*, GAMP, 1996). The instrumentation, control solutions and data acquisition were designed for pilot scale research purposes. The critical part of the research work is the possibility for rapid, but controlled changes in system.

4.3.2 Mixing, extrusion and spheronisation (I, IV)

The diluents used for pellets were dry-mixed in a high-shear Fielder granulator (T.K Fielder 25/2G) for four minutes. The pellets were manufactured by the continuous extrusion-spheronisation technique (Nica M6L mixer/granulator; Nica E140 radial screen extruder; Nica S320 spheronizer; Nica System AB, Sweden). The wet-mixed mass was extruded through a 1.25-mm screen with a length to radius (L/R)-ratio of 0.8. The spheronisation time used was three minutes and friction plate speed 900 rpm. The pellets were dried in a fluidised bed granulator (Glatt WSG 5, Glatt GmbH, Binzen, Germany).

Wet mixing (IV) was performed using a planetary mixer (Stephan UMC 5 Electronic, Stephan, Germany). The required quantity of water was added and mixed for an additional 5 minutes. Wet masses were equilibrated overnight to ensure a uniform distribution of water.

4.3.3 Compression (III)

Tablets were compressed in an instrumented eccentric tablet machine (Korsch EK0, Germany) using flat-faced 9 mm punches. The granules were mixed with 0.5 w-% magnesium stearate (Ph.Eur. 3rd Ed.) in a Turbula mixer for 5 minutes. The target compression pressure used was 100 MPa and the target weight of tablets was 295 mg. Tableting was performed in a conditioned room (35 ± 3 RH%, 24 ± 2°C).

4.4 Near-infrared spectroscopy

4.4.1 Full near-infrared off-line spectra

Near-infrared spectra were measured using an FT-NIR spectrometer (Bühler NIRVIS, Uzwil, Switzerland) with fiber-optic probe. Diffuse reflectance spectra for solids and transflectance spectra for liquids were measured over the range of 4008-9996 cm^{-1} with a resolution of 12 cm^{-1}. Each individual spectrum was an average of four scans and all measurements were performed five times. The spectral treatment (absorbances and second derivatives) was performed with NIRCAL v. 2.0 (Bühler, Uzwil, Switzerland). In this thesis, all the full spectra are referred to as FT-NIR spectra. The fixed wavelength prototypes (based on four-channel detector) are referred to as NIR set-up.

4.4.2 In-line near-infrared prototypes

Two different NIR prototypes were tested during the research. Prototype A (I, II) and B (III, VI) were both based on the integrated detector technique (Niemelä, 1988) by VTT Electronics, Optoelectronics (Oulu, Finland). The NIR prototypes were separated into two main components, the NIR probe and the main unit (Fig. 7). The optical probe was an interface between the process (fluidised bed granulator) and the main unit. The probe and the main unit were connected to each other using fiber bundles.

The chopped illumination light was coupled to a process and a collecting fiber bundle was used to collect the reflected optical signal from the process. The illumination and collecting fibers were adjusted to optimised angle in order to achieve maximum optical signal from a process. Collected, back-reflected light was coupled to detection unit, where the optics collimated it to a four-channel detector. The four-channel detector detected optical signals at four different wavelengths (moisture, baseline, and sample reference signals). The two prototypes (A and B) had different filters in four-channel detectors, and by that means, slightly different measuring wavelengths were applied.
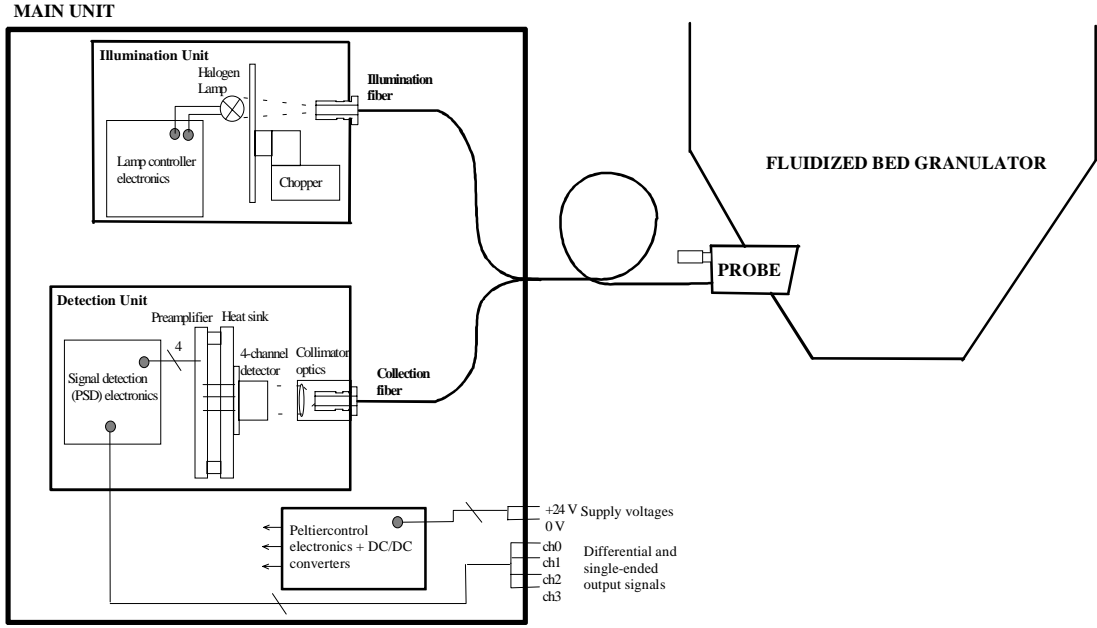
Figure 7. The structure of integrated detector NIR prototype (Suhonen, 1999).

With the NIR prototype A, the optical data (OPD) was given in the form of the following equation

$$OPD = -\log_{10}\left(\frac{\dfrac{R}{R_{ref}} - \dfrac{R_x}{R_{x,ref}}}{\dfrac{R_y}{R_{y,ref}} - \dfrac{R_x}{R_{x,ref}}}\right) \qquad (9)$$

where R, R_x and R_y are reflectances of water, background level, and non-water absorbing reference, and R_{ref}, $R_{x,ref}$, and $R_{y,ref}$ are aluminum plate references, respectively. The non-absorbing reference used was a sand-blasted aluminum plate. The 1990 nm wavelength was applied for detection of water. The 1740 nm signal was used for correction of the background level and 2145 nm was applied as a non-water-sensitive reference.

With the NIR prototype B, the baseline corrected and normalised (Mercer, 1980) apparent water absorbance (AWA) was determined as follows

$$AWA = \frac{-\log_{10}(\dfrac{I_x}{I_{x,ref}}) + \log_{10}(\dfrac{I_y}{I_{y,ref}})}{-\log_{10}(\dfrac{I_z}{I_{z,ref}}) + \log_{10}(\dfrac{I_y}{I_{y,ref}})} \qquad (10)$$

where I is intensity of reflectance (x referring to 1998 nm signal, y 1813 nm signal and z 2214 nm (AWA$_1$) or 2136 nm (AWA$_2$) signal) and ref is intensity using aluminum plate reference at the corresponding wavelength channel. The reflectance at 1998 nm was used as a water indicator. The reflectance at 1813 nm was used for baseline correction and the reflectance at 2136 or 2214 nm for normalisation.

4.5 Data analysis

4.5.1 Multivariate regression (II)

MLR analysis was used to study the dependence of one response (median of particle size, y_1) on the independent variables studied (flow rate, x_1 and drying end-point, x_2) (Modde for Windows, v. 3.0, Umetrics, Umeå, Sweden). The regression model for two independent variables was first presented as the second order polynomial (Eq. 11),

$$y_1 = a \cdot x_1 + b \cdot x_2 + c \cdot x_1 \cdot x_2 + d \cdot x_1^2 + e \cdot x_2^2 + f \qquad \textbf{(11)}$$

where a-f are coefficients. The model was then simplified with a backward selection technique, which means that terms were removed one by one so that only the significant terms ($p < 0.10$) were included in the final model.

4.5.2 Principal component analysis (III)

Principal component analysis (PCA) was used to reduce the dimensionality of the original process data matrix ($\mathbf{X}$). The process data matrix used for PCA consisted of twelve critical process measurements at 5-sec intervals. PCA was performed using SIMCA-P 7.0 software (Umetrics, Umeå, Sweden).

In PCA, the original process matrix (N x K matrix, $\mathbf{X}$) was decomposed to a set of scores, $\mathbf{T}$ (N x A matrix), describing the object variation, and a set of loadings, $\mathbf{P}$ (K x A matrix) describing the variable influence on the principal components. The non-systematic part not described by the model forms the residuals ($\mathbf{E}$). This decomposition can be described by

$$\mathbf{X} = \mathbf{TP'} + \mathbf{E} \qquad \textbf{(12)}$$

where A is the number of principal components extracted.

4.5.3 Self-organizing maps (VI)

The process data matrix was further analysed using SOM. For the training and visualisation of the SOM, a public domain Matlab (v. 5.3, The MathWorks, Inc., USA) toolbox was used (Alhoniemi et al., 1997).

By denoting x = $[x_0 \ x_1 \ ... \ x_{N-1}]^T$ (input vector) and the location vector of a mapping node by m_i = $[m_{i\ 0} \ m_{i\ 1} \ ... \ m_{i\ N-1}]^T$, the algorithm that describes the self-organizing operation is as follows:

I.   Initiate the locations of nodes with random values.

II.   For each vector of the training data compute steps III_a and III_b

III_a find the SOM node $\boldsymbol{m_c}$ (winner) best matching to the data vector x(t) by searching all nodes m_i by

$$\left\| x(t) - m_c(t) \right\| = \min_i \left\{ \ \left\| x(t) - m_i(t) \right\| \right\} \tag{13}$$

III_b adjust the locations of the nodes

$$m_i(t+1) = \begin{cases} m_i(t) + \alpha(t)\{x(t) - m_i(t)\} \ , & \textit{for } i \in N_c (= \textit{neighbourhood}) \\ m_i(t) \ , & \textit{for all other indices} \end{cases} \tag{14}$$

In Eqs. (13) and (14) the Euclidean metric can be used as the distance measure. The parameter $\alpha(t)$ in equation (14) is a coefficient that determines how much the winning node and the neighbourhood are moved in the direction of the data vector x(t).

5. RESULTS AND DISCUSSION

5.1 Data management

The critical process information during granulation was measured (Fig. 8) and the control of process parameters was performed (III). Further, the process information (the properties of process air, granulation liquid medium, and the granules) was logged and it was analysed using common software. The present set-up for process air measurement was based on the *off-line* calibration of flow tubes (III). The precise control of the process air is of importance in the manufacture of pharmaceutics, but no description of air measurements has been published before. Reliable control of process air enables reproducible performance of granulations. Process models based on mass and energy balances can be calculated if the process streams are under control.

Figure 8. The instrumentation of fluidised bed granulator.

The process trend charts during a typical granulation were plotted (III), and the different phases and subphases of granulation were identified. Visualisation of this multivariate

data is difficult. Understanding the state of the process requires granulation experience. For example, the drying endpoint is traditionally based on sampling and knowledge-based decisions made by combining information from several measurements (e.g., granule temperature, outlet air temperature, absolute humidity of outlet air, relative humidity of outlet air, NIR signals). The dimensionality of the process data was further reduced using multivariate batch modeling techniques (III, VI). Three steps of reduction are illustrated in Fig. 9. First step is the definition of critical process measurements, which describe the state of process. Altogether, these measurements compose *m* dimensional feature vector (Fig. 9, step 2). This vector is further projected to lower dimension (Fig. 9, step 3). In this study, PCA and SOM were applied for visualisation.
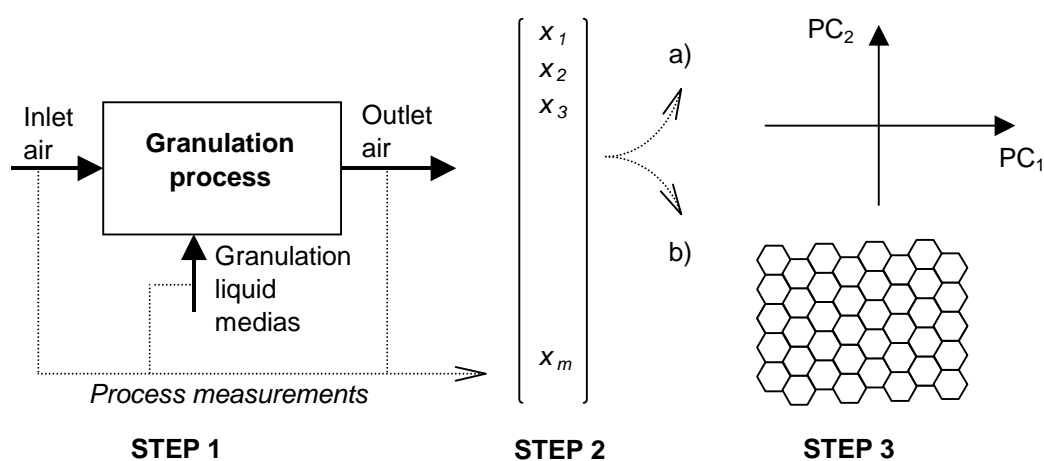
Figure 9. The reduction of dimensionality of process data (modified from Simula and Kangas, 1995); process measurements (step 1), feature vector (step 2), and process monitoring using data projection (step 3a principal component analysis; 3b self-organizing map).

The basic idea of the SCADA system described and the multivariate process monitoring can be applied to any other pharmaceutical unit operation. The critical phase of the development work is the definition of User Requirements Specifications (URS). This document should unequivocally describe the claims of the end user. The same SCADA solution was further modified and applied for automation of tablet coating pan (Ruotsalainen et al., 2000). Applying the data acquisition, process analysis and

multivariate techniques (III, VI) to other pharmaceutical unit operations results in a critically increasing amount of process data. Development of *in-line* PAC is a powerful tool when combined with multivariate techniques, but it will increase, again, the amount of process data.

The testing of structured query language (SQL) based database for data logging was performed (IndustrialSQL Server, FactorySuite 2000, Wonderware Corporation, Irvine, CA, USA) (unpublished data). The use of SQL database enables access to process information through client applications, e.g., using Intranet or Internet. Future work should concentrate on conducting similar studies on all unit operations of solid dosage form manufacture, and further, on the dependences of these stages. The development of database solution is an important part of this work.

5.2 Factors affecting the in-line moisture measurement

5.2.1 The process interface

A critical part of *non-invasive* process measurements is the interface to the process. The harsh environment in the granulator during fluid bed processing makes the development of the probe solution particularly challenging. The adhering of material may block the sight glass of the probe, and prevent the reliable measurement. Radtke et al. (1999) introduced the use of sampling device for side stream sampling in the rotary fluidised bed granulator.

In the present apparatus, the probe was installed in the conical part of the granulator and the *non-invasive* signals were measured. The sight glass of the probe was continuously blown with heated supplied air to the direction of the glass (III). The supplied air was heated with plate heat exchanger to +40°C. This set-up enabled the disturbance-free measurement.

5.2.2 Effects of chemical composition of formulation

The first prototype showed that the output of the NIR set-up (OPD signal) depended on the formulation (I). Different calibration was needed for model formulations with varying chemical composition. This was partly due to the level of absorption at the correction wavelengths (baseline and normalisation signals), partly due to the state of water at the granules. The CH related bands (first overtones) are seen at the 1600-1760

nm region (Murray and Williams, 1987), which was used for the baseline correction of the NIR set-up. Further, the non-water sensitive sample reference wavelengths used for the normalisation are at the region of various combination bands (combinations of CH, OH and CO stretches and deformations). A fixed wavelength NIR sensor (WET-EYE, Fuji Paudal, Japan) has been previously used by the group of Watano (Watano, 1995; Watano, 1996a; Watano, 1996b). Watano et al. (1996b) evaluated the formulation effects on the NIR sensor output, and they found the mixing ratio of the model formulation (lactose monohydrate: cornstarch) affecting the calibration. This was explained by the state of water in the materials used. Water absorbing potential of cornstarch was higher than that of lactose monohydrate. The same phenomenon was observed when comparing materials with different water absorbing potential (IV, Fig. 4). After same water addition, the baseline corrected and normalised absorbance values were lower with materials having higher water absorbing potential. This was due to the low penetration depth of the
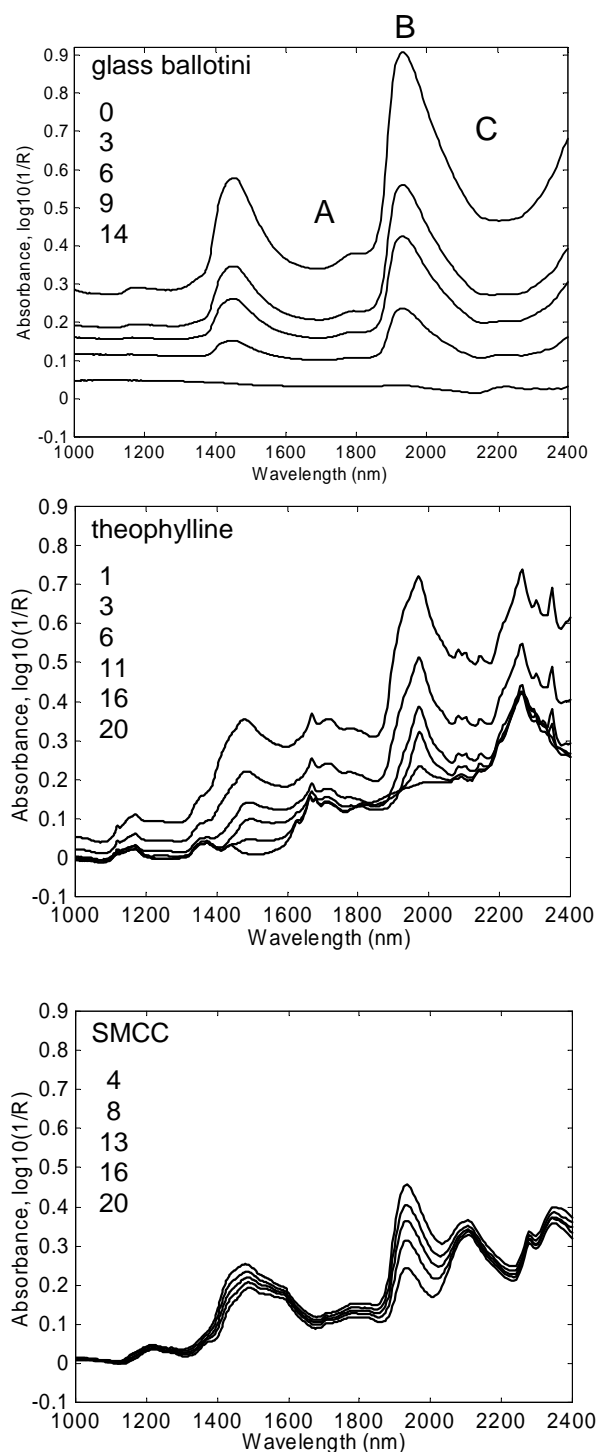
Figure 10. Effect of increasing water content (numbers referring to g of water per g of dry material) on the NIR spectra.
The wavelength regions used for NIR set-up indicated, (A) baseline correction, (B) water, (C) normalisation.

radiation, and the water at the surface of materials (glass ballotini and lactose monohydrate) was detected to more extent than the absorbed water (corn starch (Watano et al., 1996b) and SMCC). However, it is difficult to evaluate the effects of different formulations to the fixed wavelength NIR set-ups without information of the full NIR spectra (Fig. 10). The full FT-NIR spectra were used for evaluation of the calibration behaviour of model compounds, theophylline and silicified microcrystalline cellulose (III). The varying calibration behaviour of compounds was explained by differences in FT-NIR spectra at normalisation region. Theophylline had an absorbance in the 2200-2300 nm region (Fig. 10), which resulted in higher AWA_2 values (normalisation I_z from the 2136 nm signal) in comparison with AWA_1 (normalisation I_z from the 2214 nm signal) (Eq. 11). The increase in nominator resulted in a decrease in the AWA_1 value (III, Figs. 9 and 10). SMCC with absorbance in the 2050-2150 nm region but not to the same extent in the 2200-2300 nm region (Fig. 10) showed higher AWA_1 values than AWA_2 values.

The effects of typical binders (PVP and gelatin) on the NIR measurement used in granulation were studied (V). Both the binders studied showed the CH related overtone bands around 1700 nm (first overtones of CH stretches) and a weaker band around 1200 nm (second overtones of CH stretches) (Murray and Williams, 1987). Two combination bands around 2200 nm were also noticed. This region has typically combinations of CH, OH and CO stretches and deformations. Gelatin had also an NH band around 1500 nm (first overtones of NH stretches) and a combination band at about 2050 nm. With non-porous model material (glass ballotini) there was absorption due to binder both at the baseline region and at the signal normalisation region (V, Fig. 4). However, with model compound having absorbing nature these effects were decreased (V, Fig. 5). Watano et al. (1996b) studied the effect of binder (hydroxypropylcellulose) concentration on the NIR output. They found no effect of binder concentration on the calibration of NIR.

5.2.3 Effects of physical properties of the granules

When applying NIR for *in-line* analysis of material with changing properties, e.g. the powder blend during the granulation, a truly dynamically varying matrix occurs. The effect of particle size differences may be noticed on the general baseline of spectra. The baseline of apparent absorbance, $\log(1/R)$, increases when reflectance decreases due to

the larger particle size (Norris and Williams, 1983; Osborne et al., 1993). The scattering of the light diminishes and the light penetrates deeper into the solid material with larger particle size and therefore log(1/R) increases. Norris and Williams (1983) studied ground wheat samples with a mean particle size varying from 150 to 335 μm. They found the particle size effect to be greater at longer wavelengths, but more dependent on the log(1/R) level than on the wavelength.

As described in the previous chapter, the materials capable of absorbing the water at the internal structures have lower absorbance values. As MCC is capable of holding large amounts of water in the internal structures (Fielden et al., 1988), the same amount of moisture resulted in higher water bands with non-absorbing materials at moisture levels from 0.1 ml g^{-1} up (IV, Fig. 4). The change in physical properties of the sample resulted in an upward shift of the spectral baseline (III-V). This was partly due to the change in refractive index discontinuities, and partly due to the increase in particle size. In the case of inorganic test material (glass ballotini), the glass-air interfaces (refractive indexes 1.5 and 1.0, respectively) were replaced by glass-water interfaces (refractive indexes 1.5 and 1.3, respectively). This change in refractive properties increased the effective pathlength, and resulted in an apparent increase in absorbance, log(1/R), in the whole spectra. The same was observed with SMCC, but not to the same extent. Water within an inorganic test material (glass ballotini) was adsorbed and in case of an organic test material (MCC), it was absorbed within cellulose fibers. Changes in reflection and refraction properties of materials can be further described according to Snell's law and Fresnel equations. In the case of SMCC, the increase in spectral baseline was related to the state of granule growth (IV). The height of the baseline corrected water bands increased linearly at low moisture contents, thereafter achieving a plateau stage. According to mixer torque results, the plateau stage of the band heights indicates a capillary state of the liquid saturation, as defined by Newitt and Conway-Jones (1958). Miwa et al. (2000) used the NIR sensor (WET-EYE, Fuji Paudal, Japan), and evaluated the wet massing behaviour of different excipients. They classified the excipients studied into five groups according to the output of NIR sensor. The NIR sensor output was related to the inside/surface distribution of water in *at-line* samples. Further, they used this result to estimate the amount of granulation liquid needed for wet granulation.

Watano et al. (1996a) evaluated the effects of process parameters on the calibration of NIR set-up in the agitating fluid bed. They found no effects of fluidising

air velocity or temperature, agitator rotation speed, flow rate of granulation liquid, droplet size of granulation liquid or pressure of the purge air used for cleaning of sight glass. Only the extremely low flow rate of granulation liquid and high fluidising air temperature resulted in different calibration profile. They explained this phenomenon by the transfer of water from inside the granule to the surface of granule in these extreme conditions. However, with increasing temperature the absorbance maximum of water (the combination band of water, $\tilde{v}_2 + \tilde{v}_3$, around 1940 nm) occurs at lower wavelengths (Fornés and Chaussidon, 1978). This affects the calibration with fixed wavelength NIR set-ups.

The data used for the calibration of theophylline (III) was further analysed using PLS modeling (Rantanen et al., 2000). The process information at the time of sampling (n=196) was collected and combined as an 18-element vector. This vector described the conditions in the granulation chamber at the time of sampling. The samples from different phases of granulation were projected in separate clusters (Fig. 11).
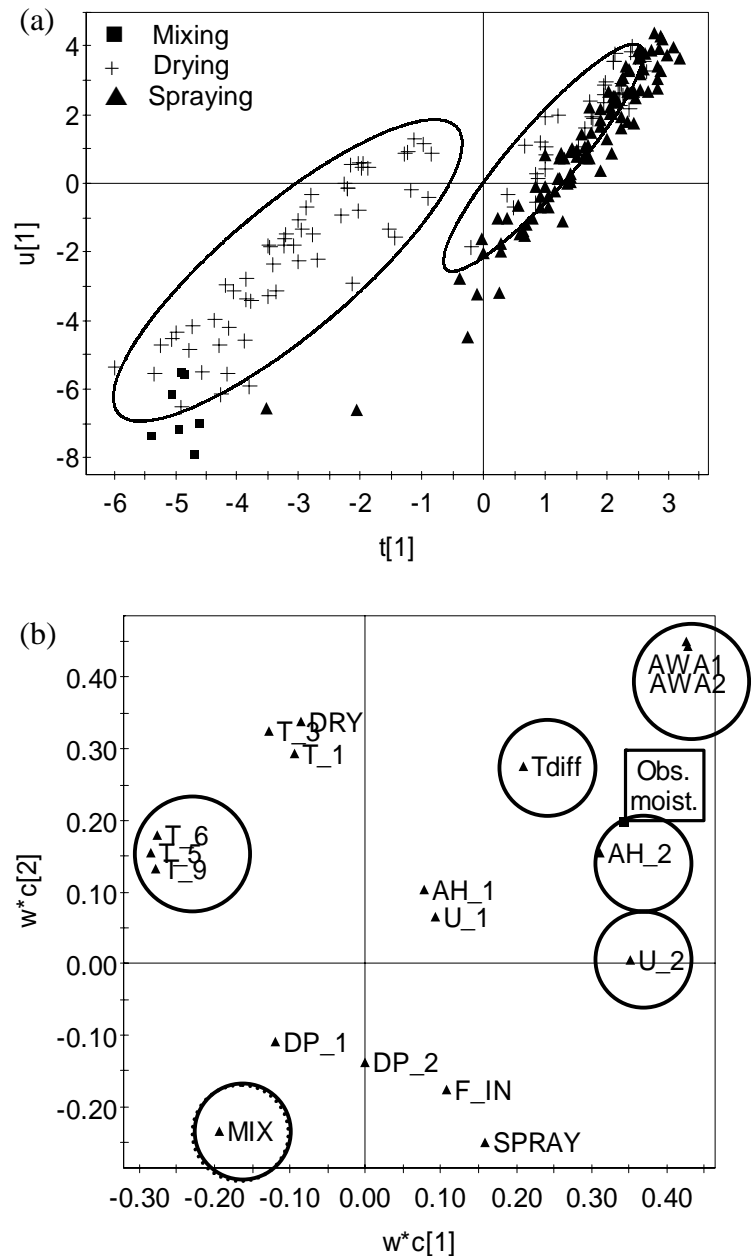
Figure 11. The PLS analysis of calibration data of theophylline (samples from different phases of granulation); (a) PLS scores, (b) PLS weights. Two groups of samples from drying phase circled in (a), and explaining variables circled with dashed line in (b) (Rantanen et al., 2000).

However, the samples collected during drying phase were divided into two groups. The explaining variables for this division were the temperature of granules and outlet air (two probes T_5 and T_6 in granulator, and one probe in outlet air channel T_9), and outlet air water content (AH_2 and U_2). In the beginning of the drying phase, all the samples were located in the smaller cluster beside the samples from spraying phase. At this phase, the temperature of granules is lower compared to the granule surface with no continuos film of granulation liquid. The superficial water on the surface of the granules was seen as a decrease in granule temperature due to the vaporisation. As the drying proceeds, the surface of the granule has no longer the continuos film of granulation liquid. This was seen as a shift in calibration. In addition, the outlet air water content is higher in the beginning of drying phase. The NIR reflectance signal from a granule with superficial water is different from that of a granule without superficial water at the end of the drying phase.

The state of water in solid material affected the NIR spectra (IV). The water of SMCC was seen as a wide water band at 1425 and 1920 nm, whereas the monohydrate of lactose was seen as a narrow water band at 1450 and 1933 nm. The broad band for absorbed water of SMCC indicates a spread of energies of interaction, whereas the monohydrate water band is typical of a more uniform interaction. Both water and SMCC affected the band at 1425 nm, since the absorbances of cellulose and water OH groups were overlapping in this region. With increasing moisture content, the water bands of SMCC shifted from 1920 nm to 1903 nm. The water band of the 1:1 mixture was seen at a slightly lower wavelength (1910 nm) than that of pure SMCC (1920 nm), and, consequently, a smaller shift from 1910 nm to 1903 nm was observed. This is due to the closeness of the monohydrate and cellulose water bands. In the case of α-lactose monohydrate and glass ballotini, the added water was seen directly at 1903 nm. The sharp monohydrate band of α-lactose at 1933 nm remained unchanged. With increasing moisture content the water bands of SMCC increased in size and shifted gradually from 1425 nm to 1410 nm. This indicates an increase in the median interaction energy of the water OH bond, since non-hydrogen-bonded OH groups have higher stretch frequencies, and hence a lower wavelength than hydrogen-bonded OH groups. The second derivative spectra of α-lactose monohydrate were capable of distinguishing hydrate water from added water. Added water resulted in a separate band at a lower wavelength (1410 nm) in comparison with the structured monohydrate band at 1450 nm.

Only a minor shift of water band, from 1415 to 1410 nm, was observed. When the energetic state of water changed from bound to bulk water, a similar water band shift was observed with the 1:1 mixture to the one with SMCC. The sharp monohydrate band at 1450 nm remained unchanged after water addition. In the case of glass ballotini, the water bands were seen directly at 1410 nm. The intensity of the water bands increased with increasing water content, while no shift could be observed. The results are consistent with Iwamoto et al. (1987) and Maeda et al. (1995), who reported that the water molecules with no hydrogen bond have a water band at 1410 nm. Also, the non-linearity of calibration of theophylline was observed (III). One reason for non-linearity with theophylline may be the pseudopolymorphic changes during processing. The formation of theophylline monohydrate during wet granulation of anhydrous theophylline has been reported (Herman et al., 1988; Räsänen et al., 2000).

5.3 The in-line NIR set-up as a tool for the process optimisation

The moistening profiles of granules and the drying end-point of granulation was measured with NIR set-up (I, II). Control of inlet air humidity is necessary in order to maintain the reproducibility of the product quality. Schæfer and Wørts (1978) showed the importance of inlet air conditions in the success of the granulation. The moistening profiles were not reproducible with the present granulator with no air handling unit (II). Variations in inlet air conditions proved critical factor explaining differences in the granule size distributions. Differences in granule moistening rates resulting from varying inlet air conditions could be measured with the NIR set-up. The moisture content of granules at the end of the spraying phase explained part of the differences in granule size distributions. The moisture content of granules at the end of the drying phase affected the tableting behaviour of granules. Residual moisture (high levels of end-point drying moisture content) resulted in a remarkable hardening of tablets compressed (II, Table 4) during 24 hours of controlled storage.

The results suggested that direct measurement of granule moisture content facilitates the in-process control of the wet granulation process. Watano (1995) applied on-off typed controller for granulation liquid pump in order to achieve desired moistening profile.

5.4 Visualisation of the granulation process

5.4.1 Principal component analysis (III)

The six granulation batches studied proceeded in a multivariate process space like through a curved tunnel (III, Fig. 6). Similar process situations (e.g. different steps of the spraying phase) were projected into the same areas of the score plot. Almost 62 % of the variation in the process data matrix was explained by the first two principal components. These two latent variables (summarising the original twelve process variables) described the state of the process in a 2D space (score plot), and the three phases (mixing, spraying, and drying) were clearly visible. Variation in score plot was due to one deviating granulation (theophylline granulation with only 2500 g of granulation liquid instead of 3000 g) and non-controllable process parameters (inlet air properties). Seasonal effects of process air (variation in relative humidity of inlet process air, U1) resulted in a deviating proceeding of the trajectory in the score plot. These effects could be visualised by creating a PCA model for the drying phase (III, Fig. 7). All drying phases proceeded from the left to the right in the score plot, but there was variation in the direction of the second component (t_2 axis). The cause for this behaviour can be found in the loading plot; the variables of major importance (resulting in the deviation in the direction of the t_2 axis) are marked with a red ellipse. The amount of granulation liquid (M_1) and inlet air properties (temperatures T_1 and T_3, and relative humidity U_1) were the variables causing the deviation between six granulation drying phases. A set of successful batches (in this case, e.g. the four granulations proceeding in about the same way in the score plot) can be used to create the multivariate statistical process control limits describing the normal operating conditions (Wold et al., 1998b).

More variation in the process data matrix could have been explained by using third (etc.) principal components. However, the process monitoring using the three first principal components must be done in 3D or using separate 2D plots (t_1 vs. t_2, t_1 vs. t_3 and t_2 vs. t_3).

5.4.2 Self-organizing maps (VI)

The SOM approach was also applied for data reduction of granulation process. Three clusters were found, corresponding to the mixing (A), spraying (B), and drying (C)

phases (VI, Fig. 6). A path taken by three granulations through the SOM is presented with an arrow. Each granulation proceeded through the map by an individual route.

The evolution through phases of granulation can be studied using the SOM. The path through the SOM presented the fingerprint of an individual granulation batch. While the overall S-shaped path through the SOM remains unchanged, the granulations proceeded in slightly different paths (VI, Fig. 6). In these experiments, the differences were due to the variation in the process inlet air. One batch (marked with red trajectory) was performed in winter, when the relative humidity of the inlet air was low. The batch proceeded through the regions of SOM with a low value of variable U_1 (VI, Fig. 7). The other two batches (marked with magenta and yellow trajectory) proceeded different routes due to the higher values of the relative humidity of the inlet air.

A successful granulation can be used to define the optimal path through the SOM (VI, Fig. 8). The deviations from this path can be used to alarm the operator. With the alarm the operator can be shown the current process state and the variable causing the deviation. In addition, the undesirable regions of the map can be defined (VI, grey areas in Fig. 8). Causes to past granulation failures can be found by studying whether the process state has visited forbidden SOM areas. For example, in the SOM presented above, such an area is in the top-left corner (VI, Fig. 8; I_a) of the drying zone. The high value of dP_1 (pressure difference over filter bags) and low value of dP_2 (pressure difference over air distribution plate and granules) indicate building up of material in filters or dead zones (immobile regions) in the granulator. Another area with an indication of filter blinding is in the low-left corner (VI, Fig. 8; I_b) of the map. The areas with low values of inlet air relative humidity can also be defined as abnormal regions (VI, Fig. 8; II_a - II_c). This information about optimal and forbidden process states is useful to the process operator. Additional benefit is gained if the operator can be suggested a correcting action. According to these results, it is evident that SOM creates a novel tool for visualisation of a complex granulation process.

5.4.3 Comparison of methods used for visualisation

Both the methods can be applied to any complex pharmaceutical unit operation with measurements describing the state of the process, e.g., in different stages of solid dosage form manufacture. Future work should concentrate on conducting similar studies on the mixing, tableting and coating processes and further, on the dependences of these stages.

The hypothesis is that the process conditions of the predecessor stages have a notable influence on the success of the successor stages.

If more than two principal components are needed for the visualisation of process with PCA, the situation is complicated. The use of 3D or parallel 2D plots is difficult. The use of the unsupervised SOM enables the 2D plotting, and all the process information is in the same plot.

6. CONCLUSIONS

Measurement system with reliable process control combined with data logging can be used for analysing the fluidised bed granulation process.

The application of near infrared reflectance spectroscopy creates a novel tool for direct and real-time measurement of water. The direct measurement of granule moisture content facilitates the in-process control of the granulation. Non-direct methods based on temperature measurements do not give exact information of the moisture content of the granules.

The four-wavelength detection proved rather limited for understanding the nature of wetting and drying during the granulation process. Future work should focus on the development of fast and simultaneous detection at a large number of measuring wavelengths. The full spectra offer the possibility to understand the nature of water-solid interactions during processing.

The PCA and SOM approach can be applied to visualisation of wet granulation of pharmaceutics. The methods are able to present the state of the granulation process and the subtle differences between various batches.

ACKNOWLEDGEMENTS

Helsinki, October 2000

REFERENCES

Aldridge, P., Evans, C., Ward, H., Colgan, S., Boyer, N. and Gemperline, P., 1996. Near-IR detection of polymorphism and process-related substances. *Anal. Chem.* **68** 997-1002.

Alhoniemi, E., Himberg, J., Kiviluoto, K., Parviainen, J. and Vesanto, J., 1997. SOM toolbox for Matlab. http://www.cis.hut.fi/projects/somtoolbox/, Helsinki University of Technology, Finland.

Andersson, M., Josefson, M., Langkilde, F. and Wahlund, K.-G., 1999. Monitoring of film coating process for tablets using near infrared reflectance spectroscopy. *J. Pharm. Biomed. Anal.* **20** 27-37.

Andersson, M., Folestad, S., Gottfries, J., Johansson, M., Josefson, M. and Wahlund, K.-G., 2000. Quantitative analysis of film coating process by in-line NIR spectrometry and multivariate batch calibration. *Anal. Chem.* **72** 2099-2108.

Axon, T., Brown, R., Hammond, S., Maris, S. and Ting, F., 1998. Focusing near infrared spectroscopy on the business objectives of modern pharmaceutical production. *J. Near Infrared Spectrosc.* **6** A13-A19.

Barnes, R., Dhanoa, M. and Lister, S., 1989. Standard normal variate transformation and de-trending of near-infrared diffuse reflectance spectra. *Appl. Spectrosc.* **43** 772-777.

Beebe, K., Blaser, W., Bredeweg, R., Chauvel, J., Harner, R., LaPack, M., Leugers, A., Martin, D., Wright, L. and Yalvac, E., 1993. Process analytical chemistry. *Anal. Chem.* **65** 199R-216R.

Bergman, R., Johansson, M., Lundstedt, T., Seifert, E. and Åberg, J., 1998. Optimization of a granulation and tabletting process by sequential design and multivariate analysis. *Chemometr. Intell. Lab. Syst.* **44** 271-286.

Berntsson, O., Zackrisson, G. and Östling, G., 1997. Determination of moisture in hard gelatin capsules using near-infrared spectroscopy: applications to at-line process control of pharmaceutics. *J. Pharm. Biomed. Anal.* **15** 895-900.

Berntsson, O., Burger, T., Folestad, S., Danielsson, L.-G., Kuhn, J. and Fricke, J., 1999. Effective sample size in diffuse reflectance near-IR spectrometry. *Anal Chem.* **71** 617-623.

Blanco, M., Coello, J., Iturriaga, H., Maspoch, S. and Rovira, E., 1997. Determination of water in ferrous lactate by near infrared reflectance spectroscopy with a fibre-optic probe. *J. Pharm. Biomed. Anal.* **16** 255-262.

Blanco, M., Coello, J., Iturriaga, H., Maspoch, S. and de la Pezuela, C., 1998. Near-infrared spectroscopy in pharmaceutical industry. *Analyst* **123** 135R-150R.

Blanco, M., Coello, J., Eustaquio, A., Iturriaga, H. and Maspoch, S., 1999. Development and validation of a method for the analysis of a pharmaceutical preparation by near-infrared diffuse reflectance spectroscopy. *J. Pharm. Sci.* **88** 551-556.

Blaser, W., Bredeweg, R., Harner, R., LaPack, M., Leugers, A., Martin, D., Pell, R., Workman, J. and Wright, L., 1995. Process analytical chemistry. *Anal. Chem.* **67** 47R-70R.

Bourquin, J., Schmidli, H., van Hoogevest, P. and Leuenberger, H., 1997. Application of artificial neural networks (ANN) in the development of solid dosage forms. *Pharm. Dev. Technol.* **2** 111-121.

Brittain, H., 1999. Methods for the characterization of polymorphs and solvates. In *Polymorphism in pharmaceutical solids*. Brittain, H. (ed.), 1st ed., New York: Marcel Dekker Inc., p 227-278.

Buckton, G., Yonemochi, E., Hammond, J. and Moffat, A., 1998. The use of near infra-red spectroscopy to detect changes in the form of amorphous and crystalline lactose. *Int. J. Pharm.* **168** 231-241.

Buice, R., Gold, T., Lodder, R. and Digenis, G., 1995. Determination of moisture in intact gelatin capsules by near-infrared spectroscopy. *Pharm. Res.* **12** 161-163.

Buijs, K. and Choppin G., 1963. Near-infrared studies of the structure of water. I. Pure water. *J. Chem. Phys.* **39** 2035-2041.

Bull, C., 1990. A model of the reflectance of near-infrared radiation. *J. Mod. Opt.* **37** 1955-1964.

Bull, C., 1991. Compensation of particle size effects in near infrared reflectance. *Analyst* **116** 781-786.

Callis, J., Illman, D. and Kowalski, B., 1987. Process analytical chemistry. *Anal. Chem.* **59** 624A-637A.

Candolfi, A., Maesschalck, R., Jouan-Rimbaud, D., Hailey, P. and Massart, D., 1999a. The influence of data pre-processing in the pattern recognition of excipients near-infrared spectra. *J. Pharm. Biomed. Anal.* **21** 115-132.

Candolfi, A., Maesschalck, R., Massart, D., Hailey, P. and Harrington, A., 1999b. Identification of pharmaceutical excipients using NIR spectroscopy and SIMCA. *J. Pharm. Biomed. Anal.* **19** 923-935.

Ciurczak, E., Torlini, R. and Demkowicz, M., 1986. Determination of particle size of pharmaceutical raw materials using near-infrared reflectance spectroscopy. *Spectroscopy* **1** 36-39.

Choppin, G. and Buijs, K., 1963. Near-infrared studies of the structure of water. II. Ionic solutions. *J. Chem. Phys.* **39** 2042-2050.

Choppin, G. and Violante, M., 1972. Near-infrared studies of the structure of water. III. Mixed solvent systems. *J. Chem. Phys.* **56** 5890-5898.

Choppin, G. and Downey, J., 1972. Near-infrared studies of the structure of water. IV. Water in relatively nonpolar solvents. *J. Chem. Phys.* **56** 5899-5904.

Curcio, J. and Petty C., 1951. The near infrared absorption spectrum of liquid water. *J. Optic. Soc. Am.* **41** 302-304.

Delwiche, S., Pitt, R. and Norris, K., 1991. Examination of starch-water and cellulose-water interactions with near infrared (NIR) diffuse reflectance spectroscopy. *Starch/Stärke* **43** 415-422.

Derksen, M., van de Oetelaar, P. and Maris, F., 1998. The use of near-infrared spectroscopy in the efficient prediction of the residual moisture of a freeze-dried product. *J. Pharm. Biomed. Anal.* **17** 473-480.

Dreassi, E., Ceramelli, G., Corti, P., Perruccio, P. and Lonardi, S., 1996. Application of near-infrared reflectance spectrometry to the analytical control of pharmaceuticals: ranitidine hydrochloride tablet production. *Analyst* **121** 219-222.

Erb, R., 1995. The backpropagation neural network – a Bayesian classifier, *Clin.Pharmacokinet.* **29** 69-79.

Fielden, K., Newton, J., O'Brien, P. and Rowe, R., 1988. Thermal studies on the interaction of water and microcrystalline cellulose. *J. Pharm. Pharmacol.* **40** 674-678.

Fornés, V. and Chaussidon, J., 1978. An interpretation of the evolution with temperature of the $v_2 + v_3$ combination band in water. *J. Chem. Phys.* **39** 2035-2041.

Frake, P., Greenhalgh, D., Grierson, S.M., Hempenstall, J.M. and Rudd, D.R., 1997. Process control and end-point determination of a fluid bed granulation by application of near infra-red spectroscopy. *Int. J. Pharm.* **151** 75-80.

Frake, P., Gill, I., Luscombe, C., Rudd, D., Waterhouse, J. and Jayasooriya, U., 1998. Near-infrared mass median particle size determination of lactose monohydrate, evaluating several chemometric approaches. *Analyst* **123** 2043-2046.

Gabrielsson, J., Nyström, Å. and Lundstedt, T., 2000. Multivariate methods in developing an evolutionary strategy for tablet formulation. *Drug Dev. Ind. Pharm.* **26** 275-296.

Good automated manufacturing practice (GAMP), 1996. Supplier guide for validation of automated systems in pharmaceutical manufacture, v. 2.0. International Society for Pharmaceutical Professionals (ISPE), Brussels, Belgium.

Geladi, P., MacDougall, D. and Martens, H., 1985. Linearization and scatter-correction for near-infrared reflectance spectra of meat. *Appl. Spectrosc.* **39** 491-500.

Goebel, S. and Steffens, K.-J., 1998. Online-messung der Produktfeuchte und Korngröße in der Wirbelschicht mit der Nah-Infrarot-Spektroskopie. *Pharm. Ind.* **60**, 889-895.

Hailey, P., Doherty, P., Tapsell, P., Oliver, T. and Aldridge, P., 1996. Automated system for the on-line monitoring of powder blending processes using near-infrared spectroscopy Part I. System development and control. *J. Pharm. Biomed. Anal.* **14** 551-559.

Han, S. and Faulkner, P., 1996. Determination of SB 216469-S during tablet production using near-infrared spectroscopy. *J. Pharm. Biomed. Anal.* **14** 1681-1689.

Hammond, J., Jee, R. and Moffat, A., 1999. Monitoring reactions in combinatorial chemistry using near-infrared reflectance spectroscopy. *J. Pharm. Pharmacol.* **51** (Supplement), 22 (abstract).

Hassel, D. and Bowman, E., 1998. Process analytical chemistry for spectroscopists. *Appl. Spectrosc.* **52** 18A-29A.

Herman, J., Remon, J., Visavarungroj, N., Schwartz, J. and Klinger G., 1988. Formation of theophylline monohydrate during the pelletisation of microcrystalline cellulose-anhydrous theophylline blends. *Int. J. Pharm.* **151** 75-80.

Herschel, W., 1800. Investigation of the powers of the prismatic colours to heat and illuminate objects; with remarks, that prove the different refrangibility of radiant heat. To which is added, an inquiry into the method of viewing the sun advantageously, with telescopes of large apertures and high magnifying powers. *Philosophical Transactions of the Royal Society* **90** 255 –283.

Hotelling, H., 1933. Analysis of a complex of statistical variables into principal components. *J. Educat. Psych.* **24** 417-441.

Hussain, A., Yu, X. and Johnson, R., 1991. Application of neural computing in pharmaceutical product development. *Pharm.Res.* **8** 1248-1252.

Hussain, A., Yu, X. and Johnson, R., 1993. Feasibility of developing a neural network for prediction of human pharmacokinetic parameters from animal data. *Pharm.Res.* **10** 466-469.

Hussain, A., Shivanand, P. and Johnson, R., 1994. Application of neural computing in pharmaceutical product development: computer aided formulation design. *Drug Dev.Ind.Pharm.* **20** 1739-1752.

Ilari, J., Martens, H. and Isaksson, T., 1988. Determination of particle size in powders by scatter correction in diffuse near-infrared reflectance. *Appl. Spectrosc.* **42** 722-728.

Iwamoto, M., Uozumi, J. and Nishinari, K., 1987. Preliminary investigation of the state of water in foods by near infrared spectroscopy. Int. NIR/NIT conference, Budapest, Hungary 3-12.

Jones, J., Last, I., Macdonald, B. and Prebble, K., 1993. Development and transferability of near-infrared methods for determination of moisture in a freeze-dried injection product. *J. Pharm. Biomed. Anal.* **11 (11/12)** 1227-1231.

Kamat, M., Lodder, R. and DeLuca, P., 1989. Near-infrared spectroscopic determination of residual moisture in lyophilized sucrose through intact glass vials. *Pharm. Res.* **6** 961-965.

Kemppainen, A., Känsäkoski, M. and Malinen, J., 1999. On-line monitoring of crispbread moisture content by short wave near infrared spectroscopy, *9th International Conference on Near-Infrared Spectroscopy*, Verona, Italy, Abstract book P. 2-7.

Kirsch, J., and Drennen, J., 1995. Determination of film-coated tablet parameters by near-infrared spectroscopy. *J. Pharm. Biomed. Anal.* **13** 1273-1281.

Kirsch, J., and Drennen, J., 1996. Near-infrared spectroscopic monitoring of the film coating process. *Pharm. Res.* **13** 234-237.

Kohonen, T., 1982. Self-organized formation of topologically correct feature maps. *Biol. Cybern.* **43** 56-69.

Kohonen, T., 1997. In *Self-organizing maps*. 2nd ed., Springer-Verlag, Heidelberg, Germany, 448 p.

Kortüm, G., 1969. In *Reflectance spectroscopy Principles, methods and applications*. 1st ed., Springer-Verlag, Berlin-Heidelberg, Germany, 366 p.

Kourti, T. and MacGregor, J., 1995. Process analysis, monitoring and diagnosis, using multivariate projection methods. *Chemometr. Intell. Lab. Syst.* **28** 3-21.

Kresta, J., MacGregor, J. and Marlin, T., 1991. Multivariate statistical monitoring of process operating performance. *Can. J. Chem. Eng.* **69** 35-47.

Last, I. and Prebble, K., 1993. Suitability of near-infrared methods for the determination of moisture in a freeze-dried injection product containing different amounts of the active ingredient. *J. Pharm. Biomed. Anal.* **11 (11/12)** 1071-1076.

Lavine, B., 1998. Chemometrics. *Anal. Chem.* **70** 209R-228R.

Lavine, B., 2000. Chemometrics. *Anal. Chem.* **72** 91R-98R.

Leiper, K., Vessman, J. and van der Vlies, C., 1998. Issues relating to the establishment of validation guidelines for material identification using NIR. *Pharmeuropa* **10** 468-470.

List, K. and Steffens, K.-J., 1996. Überwachung und Steuerung von Granulationsprozessen mit Hilfe der Nah-Infrarot-Spektroskopie. *Pharm. Ind.* **58** 347-353.

Luner, P., Majuru, S., Seyer, J. and Kemper, M., 2000. Quantifying crystalline form composition in binary powder mixtures using near-infrared reflectance spectroscopy. *Pharm. Dev. Technol.* **5** 231-246.

Luukkonen, P., Schæfer, T., Hellén, L., Juppo, A.M. and Yliruusi, J., 1999. Rheological characterization of microcrystalline cellulose and silicified microcrystalline cellulose wet masses using a mixer torque rheometer. *Int. J. Pharm.* **188** 181-192.

Maeda, H., Ozaki, Y., Tanaka, M., Hayashi, N. and Kojima, T., 1995. Near infrared spectroscopy and chemometrics studies of temperature-dependent spectral variations of water: relationship between spectral changes and hydrogen bonds. *J. Near Infrared Spectrosc.* **3** 191-201.

Martens, H. and Næs, T., 1993. In *Multivariate Calibration*. John Wiley & Sons, UK, p. 419.

Mercer, P.G., 1980. A method of measuring the content of a substance in a film comprising at least one other substance, GB Patent 2 044 443.

Merkku, P., Yliruusi, J. and Hellén, L., 1992. Testing of an automated laboratory scale fluidized bed granulator using different bed loads. *Acta Pharm. Fenn.* **101** 173-180.

Miwa A., Yajima T. and Itai S., 2000. Prediction of suitable amount of water addition for wet granulation. *Int. J. Pharm.* **195** 81-92.

Moffat, A., Trafford, A., Jee, R. and Graham, P., 2000. Meeting the international conference on harmonisation's guidelines on validation of analytical procedures: quantification as exemplified by a near-infrared reflectance assay of paracetamol in intact tablets. *Analyst* **125** 1341-1351.

Morisseau, K. and Rhodes, C., 1995. Pharmaceutical uses of near-infrared spectroscopy. *Drug Dev. Ind. Pharm.* **21** 1071-1090.

Morisseau, K. and Rhodes, C, 1997. Proven and potential uses of near-infrared spectroscopy for the evaluation of tablets. *Pharm. Technol. Yearbook 1997* 6-12.

Morris, K., Stowell, J., Byrn, S., Placette, A., Davis, T. and Peck, G., 2000. Accelerated fluid bed drying using NIR monitoring and phenomenological modeling. *Drug Dev. Ind. Pharm.* **26** 985-988.

Murray, I. and Williams, P., 1987. Chemical principles of near-infrared technology. In *Near-infrared technology in the agricultural and food industries*. Williams, P. and Norris, K. (Eds.), 1st ed., American Association of Cereal Chemists, Inc., St. Paul (MI), USA, p. 17-34.

Murtoniemi, E., Merkku, P., Kinnunen, P., Leiviskä, K. and Yliruusi, J., 1994a. The advantages by the use of neural networks in modelling the fluidized bed granulation process. *Int.J.Pharm.* **108** 155-164.

Murtoniemi, E., Merkku, P., Kinnunen, P., Leiviskä, K. and Yliruusi, J., 1994b. Effect of neural network topology and training end point in modelling the fluidized bed granulation process. *Int.J.Pharm.* **110** 101-108.

Newitt, D. and Conway-Jones, J., 1958. A contribution to the theory and practice of granulation. *Trans.Inst.Chem.Eng.* **36** 422-442.

Niemelä, P., 1988. Integrated infrared detectors for industrial process analyzers. *Proc. SPIE* **918** 80-84.

Niskanen, T., Yliruusi, J., Niskanen, M. and Kontro, O., 1990. Granulation of potassium chloride in fluidized bed granulator – Part I: Effect of flow rate. *Acta Pharm. Fenn.* **99** 13-22.

Nomikos, P. and MacGregor, J., 1995. Multivariate SPC charts for monitoring of batch processes. *Technometrics* **37** 41-59.

Norris, T., Aldridge, P. and Sekulic, S., 1997. Determination of end-points for polymorphic conversions of crystalline organic compounds using on-line near-infrared spectroscopy. *Analyst* **122** 549-552.

Norris, K. and Williams, P., 1983. Optimization of mathematical treatment of raw near-infrared signal in the measurement of protein in hard red spring wheat. I. Influence of particle size. *Cereal Chem.* **61** 158-165.

O'Neil, A., Jee, R. and Moffat, A., 1998. The application of multiple linear regression to the measurement of the median particle size of drugs and pharmaceutical excipients by near-infrared spectroscopy. *Analyst* **123** 2297-2302.

O'Neil, A., Jee, R. and Moffat, A., 1999. Measurement of cumulative particle size distribution of microcrystalline cellulose using near infrared reflectance spectroscopy. *Analyst* **124** 33-36.

Osborne, B.G., Fearn, T. and Hindle, P.H., 1993. In *Practical NIR Spectroscopy with Applications in Food and Beverage Industry Analysis*. 2nd ed., Longman, Harlow, UK, 227 p.

Padgett, M., Josephson, E., White, C. and Duffield, D., 1995. *Proceedings of the SPIE - The International Society for Optical Engineering* **2492** 562-72.

Pearson, K., 1901. On lines and planes of closest fit to systems of points in space. *Philos. Mag. Ser.* **6:2** 559-572.

Plugge, W. and van der Vlies, C., 1993. Near-infrared spectroscopy as an alternative to assess compliance of ampicillin trihydrate with compendial specifications. *J. Pharm. Biomed. Anal.* **11** 435-442.

Plugge, W. and van der Vlies, C., 1996. Near-infrared as a tool to improve quality. *J. Pharm. Biomed. Anal.* **14** 891-898.

Radtke, G., Knop, K. and Lippold, P., 1999. In-process control of direct pelletisation in the rotary fluidised bed granulator using NIR spectroscopy. *NIR news* **10** 4-12.

Rantanen, J. and Yliruusi J., 1998. Determination of particle size in a fluidized bed granulator with a near infrared (NIR) set-up. *Pharm. Pharmacol. Commun.* **4** 73-75.

Rantanen, J., Antikainen, O., Räsänen, E., Mannermaa, J-P and Yliruusi, J., 2000. Neural net model for the calibration of near infrared moisture measurement during fluidized bed granulation. *Pharmaceutical Technology 19th Conference and Exhibition*, 11.-13.4.2000, Baveno-Stresa, Italy.

Reader's tribune, 1999. Near IR spectrometry. *Pharmeuropa* **11** 275-276.

Reader's tribune, 2000. Near IR spectrometry. *Pharmeuropa* **12** 26-27.

Reeves, J., III, 1994. Effects of water on the spectra of model compounds in the short-wavelength near infrared spectral region (14000-9091 cm^{-1} or 714-1100 nm). *J. Near Infrared Spectrosc.* **2** 199.

Rowe, R. and Roberts, R., 1998. In *Intelligent software for product formulation*. Taylor & Francis Ltd, London, UK, 250.

Ruotsalainen, M., Heinämäki, J., Rantanen, J., Konttinen, P., Lauronen, E. and Yliruusi, J., 2000. Design and testing of an instrumentation system for aqueous film coating of targets in a side-vented pan coater. *Pharmaceutical Technology 19th Conference and Exhibition*, 11.-13.4.2000, Baveno-Stresa, Italy.

Räsänen, E., Rantanen, J., Jørgensen, A., Karjalainen, M., Paakkari, T. and Yliruusi, J., 2000. Novel identification of pseudopolymorphic changes of theophylline during wet granulation using near infrared spectroscopy. *J. Pharm. Sci.* (accepted for publication).

Savitzky, A. and Golay, M., 1964. Smoothing and differentiation of data by simplified least squares procedures. *Anal. Chem.* **36** 1627-1639.

Schæfer, T. and Wørts, O., 1978. Control of fluidized bed granulation III. Effect of inlet air temperature and liquid flow rate on granule size and size distribution. Control of moisture content of granules in the drying phase. *Arch. Pharm. Chemi. Sci.* **6** 1-13.

Sekulic, S., Ward, H., Brannegan, D., Stanley, E., Evans, C., Sciavolino, S., Hailey, P. and Aldridge, P., 1996. On-line monitoring of powder blend homogeneity by near-infrared spectroscopy. *Anal.Chem.* **68** 509-513.

Simula, O. and Kangas, J., 1995. In *Neural Networks for Chemical Engineers*. Bulsari, A. (Ed.), Elsevier Science, Amsterdam, p. 371-384.

Sinsheimer, J. and Poswalk, N., 1968. Pharmaceutical applications of the near infrared determination of water. *J. Pharm. Sci.*, **57** 2007-2010.

Sjöblom, J., Svensson, O., Josefson, M., Kullberg, H. and Wold, S., 1998. An evaluation of orthogonal signal correction to calibration transfer of near infrared spectra. *Chemometr. Intell. Lab. Syst.* **42** 229-244.

Skelly, J., van Buskirk, G., Savello, D., Amidon, G., Arbit, H., Dighe, S., Fawzi, M., Gonzalez, M., Malick, A., Malinowski, H., Nedich, R., Peck, G., Pearce, D., Shah, W., Shangraw, R., Schwartz, J. and Truelove, J., 1993. Scaleup of immediate release oral solid dosage forms. *Pharm. Res.* **10** 313-316.

Suhonen, J., 1999. Technical description - Multi-channel NIR sensor for moisture measurements. Technical note, VTT Electronics (Oulu, Finland).

Svensson, O., Josefson, M. and Langkilde, F., 1999. Reaction monitoring using Raman spectroscopy and chemometrics. *Chemometr. Intell. Lab. Syst.* **49** 49-66.

Švedas, V., 2000. Transformation of the near-infrared bands of cellulose surface hydroxyls under the influence of adsorbed water molecules. *Appl. Spectrosc.* **54** 420-425.

Tryba, V. and Goser, K., 1991. Self-Organizing Feature Maps for Process Control in Chemistry. In *Artificial Neural Networks, Proc. ICANN*. T. Kohonen, K. Mäkisara, O. Simula and J. Kangas (Eds.), North-Holland, Amsterdam, Netherlands, p. 847-852.

Trygg, J. and Wold, S., 1998. PLS regression on wavelet compressed NIR spectra, *Chemometr. Intell. Lab. Syst.* **42** 209-220.

Watano, S., Terashita, K. and Miyanami, K., 1990. Development and application of infrared moisture sensor to complex granulation. *Bull. Univ. Osaka. Pref., Series A* **39** 187-197.

Watano, S., 1995. *Mechanism and control of granule growth in fluidized bed granulation.* Ph.D. Thesis, Collage of Engineering, University of Osaka, Japan, 171 p.

Watano, S. Takashima, H. Sato, Y., Yasutomo, T. and Miyanami, K., 1996a. Measurement of moisture content by IR sensor in fluidized bed granulation. Effects of operating variables on the relationship between granule moisture content and absorbance IR spectra. *Chem. Pharm. Bull.* **44** 1267-1269.

Watano, S., Takashima, H., Sato, Y., Miyanami, K. and Yasutomo, T., 1996b. IR absorption characteristics of an IR moisture sensor and mechanism of water transfer in fluidized bed granulation. *Advanced Powder Technol.* **7** 279-289.

Watano, S., Takashima, H. and Miyanami, K., 1997a. Control of moisture content in fluidized bed granulation by neural network. *J.Chem.Eng.Jpn.* **30** 223-229.

Watano, S., Sato, Y. and Miyanami, K., 1997b. Application of neural network to granulation scale-up. *Powder Technol.* **90** 153-159.

White, J., 1994. On-line moisture detection for a microwave vacuum dryer. *Pharm. Res.* **11** 728-732.

Williams, P., 1987. Variables affecting near-infrared reflectance spectroscopic analysis. In *Near-infrared technology in the agricultural and food industries*. Williams, P. and Norris, K. (Eds.), 1st ed., American Association of Cereal Chemists, Inc., St. Paul (MI), USA, p. 143-167.

Wold, S., 1995. Chemometrics; what do we mean with it, and what do we want from it? *Chemometr. Intell. Lab. Syst.* **30** 109-115.

Wold, S., Antti, H., Lindgren, F. and Öhman, J., 1998a. Orthogonal signal correction of near-infrared spectra. *Chemometr. Intell. Lab. Syst.* **42** 175-185.

Wold, S., Kettaneh N., Fridén H. and Holmberg A, 1998b. Modelling and diagnostics of batch processes and analogous kinetic experiments. *Chemometr. Intell. Lab. Syst.* **44** 331-340.

Workman, J., Jr., Veltkamp, D., Doherty, S., Anderson, B., Creasy, K., Koch, M., Tatera, J., Robinson, A., Bond, L., Burgess, L., Bokerman, G., Ullman, A., Darsey, G., Mozayeni, F., Bamberger, J. and Greenwood, M., 1999. Process analytical chemistry. *Anal. Chem.* **71** 121R-180R.

Workman, J., Jr., 1993. A review of process near infrared spectroscopy: 1980-1994. *J. Near Infrared Spectrosc.* **1** 221-245.

Vrettos, N. and Hofmann, V., 1996. Optimizing the manufacture structures of international pharmaceutical companies Part I: The importance of production. *Drugs made in Germany* **39** 71-75.

Vrettos, N. and Hofmann, V., 1997. Optimizing the manufacture structures of international pharmaceutical companies Part II: Optimizing production sites. *Drugs made in Germany* **40** 43-48.

Yoon, W., Jee, R. and Moffat, A. 1998. Optimisation of sample presentation for the near-infrared spectra of pharmaceutical excipients. *Analyst* **123** 1029-1034.

Yoon, W., Jee, R., Moffat, A., Blackler, P., Yeung, K. and Lee, D., 1999. Construction and transferability of a spectral library for the identification of common solvents by near-infrared transflectance spectroscopy. *Analyst* **124** 1197-1203.